

Estuary Trophic Index Bayesian Belief Network: structure and conditional probability table description

Prepared for ETI Tool 3

November 2020

Prepared by:

John Zeldis
David Plew

For any information regarding this report please contact:




John Zeldis
Principal Scientist Marine Ecology
Marine
+64-3-348 8987
john.zeldis@niwa.co.nz

National Institute of Water & Atmospheric Research Ltd
PO Box 8602
Riccarton
Christchurch 8011

Phone +64 3 348 8987

NIWA CLIENT REPORT No: 2020276CH
Report date: November 2020
NIWA Project: FWWQ2001

Revision	Description	Date
Version 1.0	Final Report	25 November 2020

Quality Assurance Statement		
	Reviewed by:	Bruce Dudley
	Formatting checked by:	Rachel Wright
	Approved for release by:	Helen Rouse

© All rights reserved. This publication may not be reproduced or copied in any form without the permission of the copyright owner(s). Such permission is only to be given in accordance with the terms of the client's contract with NIWA. This copyright extends to all forms of copying and any storage of material in any kind of information retrieval system.

Whilst NIWA has used all reasonable endeavours to ensure that the information contained in this document is accurate, NIWA does not give any express or implied warranty as to the completeness of the information contained herein, or that it will be suitable for any purpose(s) other than those specifically contemplated during the Project or agreed by NIWA and the Client.

Contents

Executive summary	6
1 Introduction: New Zealand Estuary Trophic Index (ETI)	7
2 ETI Tool 3: Bayesian Belief Network	9
3 Descriptions and derivations of conditional probability tables (CPTs)	14
3.1 Salinity / potential total N concentration / macroalgal EQR	14
3.2 Potential TN concentration / flushing / salinity / phytoplankton.....	16
3.3 Percent intertidal/primary indicators score	21
3.4 Estuary type / closure duration / sediment trapping efficiency.....	21
3.5 Sediment load / sediment trapping efficiency / sediment deposition	25
3.6 Sediment deposition / mud	26
3.7 Macroalgae / mud / sediment TOC	27
3.8 Macroalgae / TOC / sediment apparent Redox Potential Discontinuity	29
3.9 Macroalgae / mud / TOC / macrobenthos.....	32
3.10 Stratification / estuary type / flushing / phytoplankton / oxygen.....	34
3.11 Potential N concentration / mud / seagrass.....	41
3.12 Indicator nodes / standardised nodes	43
3.13 Standardised primary nodes / ETI primary score	44
3.14 Standardised secondary nodes / ETI secondary score	44
3.15 ETI primary score and ETI secondary score / ETI final score	44
4 Example BBN results	45
5 Acknowledgements	48
6 References	49

Tables

Table 2-1:	Ecological conditions associated with the bandings (A – D) of the ETI final score (0 – 1) in the BBN.	10
Table 2-2:	BBN nodes, units and definitions.	11
Table 2-3:	Background knowledge for the Conditional Probability Tables (CPTs) underpinning the BBN.	13
Table 3-1:	Predicted effects of salinity and potential total nitrogen (TN) concentration on macroalgal Ecological Quality Rating (EQR) in NZ estuaries.	16

Table 3-2:	Predicted effects of seasonality factor, estuary flushing time (d) and potential TN concentration (mg/m ³) on phytoplankton concentrations (mg/m ³) in NZ estuaries.	18
Table 3-3:	Mapping of predicted phytoplankton concentrations (Table 3-2) to ETI Primary scores (0-16).	20
Table 3-4:	Frequency distributions of trapping efficiency for each ETI estuary type, in their open state.	24
Table 3-5:	Trapping efficiencies for SIDE and SSRTRE with short and long closure.	24
Table 3-6:	Predicted effects of estuary type and estuary closure state on estuary sediment trapping efficiency.	24
Table 3-7:	Predicted effects of estuary sediment trapping efficiency and sediment load on estuary sediment deposition rate.	26
Table 3-8:	Predicted effects of estuary sediment deposition on estuary %mud.	27
Table 3-9:	Predicted effects of macroalgal EQR on %TOC.	28
Table 3-10:	Predicted effects of %mud on %TOC.	29
Table 3-11:	Predicted effects of macroalgal EQR and %mud on %TOC.	29
Table 3-12:	Predicted effects of %TOC on aRPD.	30
Table 3-13:	Relationships between aRPD, macroalgal dry weight, macroalgal wet weight and EQR.	31
Table 3-14:	Predicted effects of EQR on aRPD.	31
Table 3-15:	Predicted effects of EQR and %TOC on aRPD.	32
Table 3-16:	Predicted effects of macroalgal EQR, %TOC and %mud on AMBI Biotic Coefficients (BC's).	33
Table 3-17:	Ecological conditions associated with the bandings (A – D) of the Oxygen node of the BBN.	36
Table 3-18:	Predicted effects of stratification and estuary type on O ₂ depletion susceptibility.	39
Table 3-19:	Predicted effects of O ₂ depletion susceptibility, chl- <i>a</i> biomass (mg/L) and estuary flushing time (d) on estuary O ₂ levels (mg/L).	39
Table 3-20:	Predicted effects of Potential Total Nitrogen concentration (mg/m ³) and %mud on seagrass.	43
Table 3-21:	Example mapping of predicted macroalgal EQR to the range of ETI Primary scores (0-16).	44

Figures

Figure 2-1:	Schematic of the ETI Tool 3 Bayesian Belief Network (BBN).	9
Figure 3-1:	Observations of macroalgae Ecological Quality Rating (EQR) plotted against potential total nitrogen (TN) concentrations for 21 NZ estuaries.	15
Figure 3-2:	Contours of predicted chlorophyll- <i>a</i> (chl- <i>a</i>) concentrations (µg/l) as a function of the potential total nitrogen concentration and estuary flushing time.	17
Figure 3-3:	Conceptual diagram of an estuary showing the terms in the sediment mass balance model.	22
Figure 3-4:	Relationship of %mud and %TOC in five Southland SIDE and SSRTRE estuaries.	28
Figure 3-5:	Sediment %TOC vs aRPD.	30

Figure 3-6:	Apparent oxygen utilisation (AOU: mg/L) results from the biophysical mooring at the outer (40 m depth) Firth of Thames location, from 2011 to 2017.	39
Figure 4-1:	Netica BBN output for Jacobs River Estuary in its current state.	45
Figure 4-2:	Netica BBN output for Jacobs River Estuary with potential TN concentration reduced by 66%.	46
Figure 4-3:	Netica BBN output for Bluff Harbour in its current state.	47

Executive summary

Excessive nutrient input (eutrophication) and elevated sediment inputs threaten many Aotearoa New Zealand (NZ) estuaries, causing ecological problems such as algal blooms and poor physical and chemical conditions for estuarine life. Until recently, guidance on how to assess the extent of eutrophication and sediment impacts in NZ estuaries was limited. To respond to this challenge, regional councils worked with NIWA to develop the Estuary Trophic Index (ETI) tools.

The purpose of the ETI is to provide ‘a nationally consistent approach to the assessment and prediction of estuary eutrophication’. Three ETI tools were built, and were provided within three Web-based applications:

- Tool 1: Determining eutrophication susceptibility using physical and nutrient load data
- Tool 2: Assessing Estuary Trophic State using measured trophic indicators
- Tool 3: Assessing Estuary Trophic State using a Bayesian Belief Network

The ETI has adopted a simple four-category typology specifically suited to the assessment of estuarine eutrophication susceptibility in NZ: coastal lake (normally closed to the sea), shallow intertidally dominated estuary (SIDE), shallow short residence-time tidal river estuary (SSRTRE), and deep sub-tidally dominated estuary (DSDE). These use of these four estuary types reflects the fact that estuary trophic responses are often related to estuary physiographic characteristics.

The ETI tools enable users to assess susceptibility of estuaries to eutrophication (Tool 1) and score an estuary along an ecological gradient from minimal to high eutrophication using field observations of indicator states collected from estuary surveys (Tool 2). This report provides details of Tool 3, which is a Bayesian Belief Network (BBN) description of estuary response to eutrophication and sedimentation pressure. The BBN predicts ETI scores using the same scoring algorithm as employed in ETI Tool 2 and uses input derivable from ETI Tool 1.

This report describes the overall structure of the Tool 3 BBN and the ecological and physiographic information underpinning the connections between its nodes. These are accumulated from knowledge based on NZ and international estuarine science and are compiled almost exclusively using either observation-based or model-derived information, with minimal reliance on expert opinion. The aim of the report is to provide users of the BBN with the rationale of the BBN structure and to facilitate its use.

The report concludes by demonstrating the utility of the BBN in examples applied to impacted and un-impacted estuaries. These show that several estuary health indicators, as well as the final integrated ETI estuary health score, may be predicted solely based on the inputs (drivers) which are available from ETI Tool 1. This means that estuary health status may be predicted in the absence of within-estuary indicator values should these not be available. Should indicator values be available, the BBN has the feature of allowing the user to update their respective nodes, which is expected to improve the accuracy of downstream indicator predictions and the final ETI health score. Finally, the examples show how scenarios may be tested, including how changed catchment nutrient loading rates affect estuary health indices.

1 Introduction: New Zealand Estuary Trophic Index (ETI)

Excessive nutrient input (eutrophication) and elevated sediment inputs threaten many Aotearoa New Zealand (NZ) estuaries, causing ecological problems such as algal blooms and poor physical and chemical conditions for estuarine life. The problems arise because the nutrients affect the trophic condition of the estuary, essentially overfeeding the algae, causing very high growth and poor oxygen and other conditions as the algae respire and decay. In addition, and often synergistically, excessive fine sediment inputs act to physically disturb biotic habitat and exacerbate nutrient retention and eutrophication. Until recently, guidance on how to assess the extent of eutrophication and sediment impacts in NZ estuaries was limited. This made it difficult to determine the current trophic state of estuaries, or to assess the impact of freshwater nutrient and sediment loads on trophic state. In turn, this has made it challenging to predict the consequences for estuaries of management decisions regarding land-use and point source discharges or setting nutrient limits for upstream environments.

To respond to these challenges, regional councils worked with NIWA to develop the Estuary Trophic Index (ETI) project, using the 'Envirolink Tools' funding pathway of the Ministry of Business, Innovation and Employment (MBIE). The ETI was delivered in 2017 by a team comprised of NIWA marine ecologists and modellers, Wriggle Coastal Management staff, regional council coastal scientists and a scientist from Hume Consulting.

The purpose of the ETI is to provide 'a nationally consistent approach to the assessment and prediction of estuary eutrophication'. Three ETI tools were built, enabling users to assess susceptibility of estuaries to eutrophication based on their nutrient/sediment loads and their flushing/dilution characteristics (Tool 1), and to score an estuary along an ecological gradient from minimal to high eutrophication using values of monitored indicators derived from field surveys (Tool 2). Tool 3, on the other hand, is a predictive tool for scoring estuary health which combines products and attributes of Tools 1 and 2, to enable users to determine estuary health in the absence of detailed knowledge of indicator states, or to scenario-test effects of changed upstream loading or land use on estuary health.

The ETI provides these capabilities within three Web-based applications:

- Tool 1: Determining eutrophication susceptibility using physical and nutrient load data
- Tool 2: Assessing Estuary Trophic State using measured trophic indicators
- Tool 3: Assessing Estuary Trophic State using a Bayesian Belief Network

The applications provide the users with instructions for use of the tools, and background material and references describing their underpinning science. Links to all three tools may be found at [ETI Tool 1: Determining susceptibility of estuaries to eutrophication \(niwa.co.nz\)](#).

This report provides details of Tool 3 of the ETI, which is a Bayesian Belief Network (BBN) description of estuary response to eutrophication and sedimentation pressure (Zeldis et al. 2017b). BBNs are particularly useful for identifying and resolving complex environmental problems because they can incorporate the effects of multiple influences on values (in this case, ecological values) and can include information from a variety of sources, including empirical data, various types of models, literature and expert opinion while handling their uncertainty (Quinn et al. 2013; Uusitalo 2007). The ETI BBN was developed within the software package NETICA (Norsys 2005). It is presented as a graphical depiction of the system key factors (nodes) and their conditional dependencies indicated by arrows connecting 'parent' and 'child' nodes (Uusitalo 2007). The relationships between linked

nodes are quantified by conditional probability tables (CPTs) to estimate the probabilities of the state of child nodes, based on states of their parent nodes using Bayes Theorem and the chain rule of probability theory.

The Tool 3 BBN predicts ETI scores, using the same scoring algorithm as employed in ETI Tool 2 (Zeldis et al. 2017c), and using input derivable from ETI Tool 1 (Zeldis et al. 2017a). The instructions available at the Tool 3 web application guide users on use of the Tool; here we describe how ecological and physiographic knowledge was implemented in its construction. The aim of the report is to provide users of the ETI Tool 3 BBN with the rationale of the BBN structure, to facilitate its use.

All three ETI tools resolve their predictions based on estuary eco-morphological type. This accounts for the variable influence of estuary physiography in determining the expression of eutrophication (Cloern 2001; Cloern and Jassby 2008; Ferreira et al. 2005; Hughes et al. 2011; Monbet 1992; NRC 2000). The ETI has adopted a simple four-category typology specifically suited to the assessment of estuarine eutrophication susceptibility in NZ: coastal lake (normally closed to the sea), shallow intertidally dominated estuary (SIDE, i.e., lagoon estuaries), shallow to moderately deep, short residence-time tidal river estuary (SSRTRE, i.e., river mouth estuaries), and deep sub-tidally dominated estuary (DSDE, i.e., deep bays and fiords). Subtypes of SIDEs and SSRTREs that intermittently close to the sea are referred to as intermittently closed and open estuaries (ICOE). The ETI typology is a simplification of the more finely - resolved NZ Coastal Hydrosystem classification (NZCH) of Hume et al. (2016) and the relationships of the estuary types in the ETI and NZCH are described in Hume (2018).

2 ETI Tool 3: Bayesian Belief Network

The ETI Tool 3 BBN (Figure 2-1) uses knowledge of the ecological connections between drivers of estuary trophic condition (e.g., estuary type, nutrient and sediment loads, flushing rate, stratification etc.) and responses of indicators (e.g., macroalgal/phytoplankton biomass, muddiness, macrobenthic and seagrass health, oxygen levels etc.) to calculate the ETI score. The drivers and indicators used are those included in Tools 1 and 2, enabling Tool 3 predictions to be directly compared with Tool 1 and 2 outputs.

ETI Tools 2 and 3 distinguish these indicators into ‘primary’ and ‘secondary’ indicators, to describe (respectively) whether they are responses of primary producers (i.e., macroalgal and phytoplankton biomasses) or responses of estuary health ‘symptoms’ (e.g., macrobenthic health, muddiness, sediment carbon, oxygen, seagrass extent). This distinction determines how their scores are combined into the final ETI score, where the maximum of the primary indicators is combined with the average scores of the secondary indicators. The ecological conditions associated with the bandings (A - D) of the ETI final score (Robertson et al. 2016b) are described in Table 2-1.

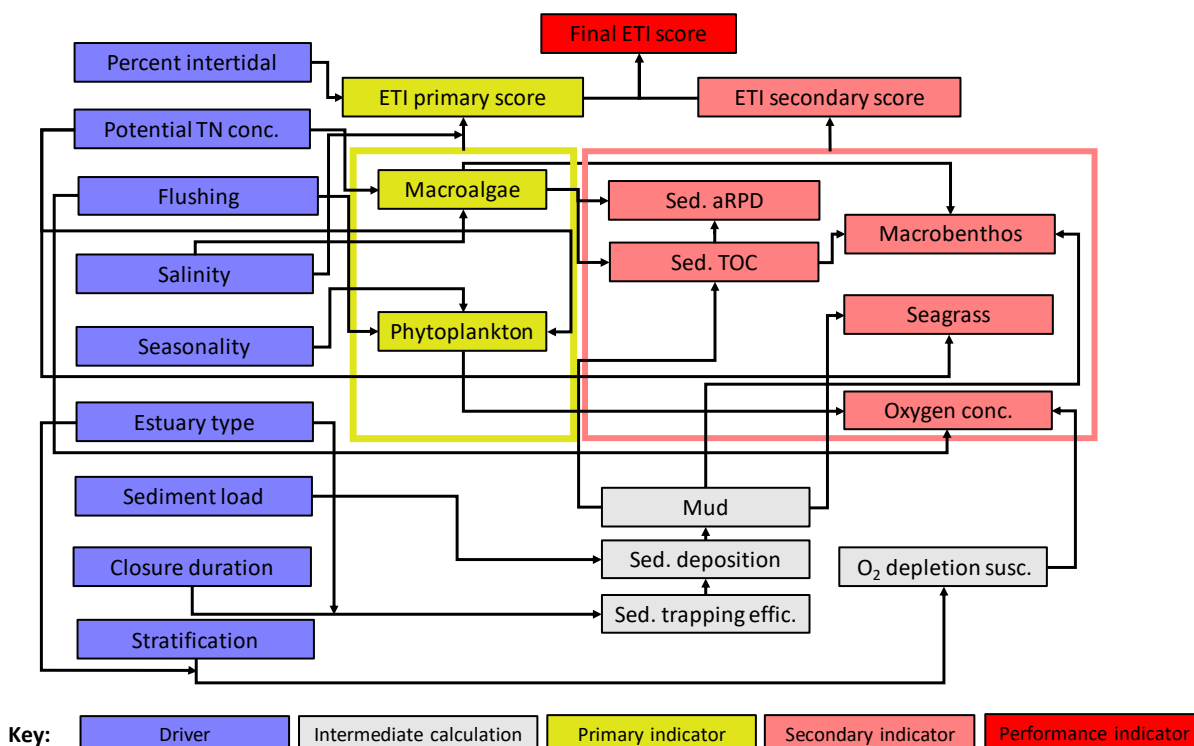


Figure 2-1: Schematic of the ETI Tool 3 Bayesian Belief Network (BBN). Information for driver nodes (blue nodes) are input by the user and the BBN calculates states of primary and secondary trophic indicators (green and pink nodes, respectively). Primary and secondary indicator values are used to produce ETI primary and secondary scores, respectively, which are then combined to give the final ETI performance score (red node). Some secondary nodes are calculated using intermediate calculation nodes (grey nodes) which do not directly contribute secondary indicator scores. All driver node values are available from ETI Tool 1 output, except for stratification, which is decided by the user. For brevity, nodes used for standardising values of primary and secondary indicators prior to input to primary and secondary score nodes are not shown here but are summarised by green and pink rectangles, respectively (see section 3.12). BBN components are further defined in Table 2-2.

Table 2-1: Ecological conditions associated with the bandings (A – D) of the ETI final score (0 – 1) in the BBN. *indicates applicable to shallow estuaries, i.e., SIDs, SSRTREs, coastal lakes; ** indicates applicable to moderate to deep subtidal dominated estuaries, i.e., DSDEs (adapted from Robertson et al. (2016b)).

Band A 0 – 0.25	Band B >0.25 – 0.5	Band C >0.5 – 0.75	Band D >0.75 – 1
<p>Ecological communities are healthy and resilient.</p> <p>*Primary producers: dominated by seagrasses and microalgae.</p> <p>**Primary producers: dominated by phytoplankton (diverse, low biomass). Water Column: high clarity, well-oxygenated. Sediment: well oxygenated, low organic matter, low sulphides and ammonium, diverse macrofaunal community with low abundance of enrichment tolerant species.</p>	<p>Ecological communities are slightly impacted by additional algal growth arising from nutrient levels that are elevated.</p> <p>*Primary producers: seagrass/ microalgae still present but increasing biomass of opportunistic macroalgae.</p> <p>**Primary producers: dominated by phytoplankton (moderate diversity and biomass). Water column: moderate clarity, moderate - poor DO especially at depth. Sediment: moderate oxygenation, organic matter, and sulphides, diverse macrofaunal community with increasing abundance of enrichment tolerant species.</p>	<p>*Ecological communities are highly impacted by macroalgal or phytoplankton biomass elevated well above natural conditions. Conditions likely to affect habitat available for native macrophytes.</p> <p>**Ecological communities are highly impacted by phytoplankton biomass elevated well above natural conditions. Reduced water clarity may affect deep seagrass beds.</p> <p>*Primary producers: opportunistic macroalgal biomass high, seagrass cover low. Increasing phytoplankton where residence time long.</p> <p>**Primary producers: dominated by phytoplankton (low diversity and high biomass). Water column: low-moderate clarity, low DO, especially at depth. Sediment: poor oxygenation, high organic matter and sulphides, macrofauna dominated by high abundance of enrichment tolerant species.</p>	<p>*Excessive algal growth making ecological communities at high risk of undergoing a regime shift to a persistent, degraded state without macrophyte / seagrass cover.</p> <p>**Excessive algal growth making ecological communities at high risk of undergoing a regime shift to a nuisance algal bloom situation.</p> <p>*Primary producers: opportunistic macroalgal biomass very high or high/low cycles, no seagrass. Cyanobacterial mats may be present.</p> <p>**Primary producers: may be dominated by nuisance phytoplankton (e.g., cyanobacteria, picoplankton). Water column: low clarity, deoxygenated at depth. Sediment: anoxic, very high organic matter and sulphides, subsurface macrofauna very limited or absent.</p>

The definitions and derivations of the drivers and indicators are given in Table 2-2. The drivers and indicators are considered as ‘nodes’ within the BBN model; this report details the information underpinning the connections between these nodes. The information has been accumulated from local knowledge based on NZ and international estuarine science (summarised in Table 2-3) and is used to determine a) relationships of drivers to indicator responses and b) the probabilities that various states of the drivers will cause the indicators to occupy different states. These probabilities are described with conditional probability tables (CPTs) in the BBN, described in this report.

In this work, nearly all the relationships between these nodes have been determined using observation - based or model - derived information, rather than with a strong reliance on expert opinion. Although use of expert opinion is a recognised and valid method of informing BBN models (Uusitalo 2007) we considered it preferable to rely, whenever possible, on more objectively - determined relationships.

Table 2-2: BBN nodes, units and definitions.

Node	Unit	Definitions
Salinity	psu	Estuary average salinity. Obtained from Tool 1 using dilution modelling (Plew et al. 2018).
Percent intertidal	%	% of the estuary that is intertidal. Ranges from 0 - 100. Obtained from Tool 1, originally from the Coastal Explorer database (Hume et al. 2007).
Potential TN concentration	mg/m ³	Estuary average TN concentration in absence of non-conservative fluxes (plant uptake, denitrification). Obtained from Tool 1 using dilution modelling (Plew et al. 2018).
Flushing	days	Time required for the freshwater inflow to equal the amount of freshwater originally in the water body. Obtained from Tool 1 using dilution modelling (Plew et al. 2018). The BBN uses a flushing time calculated for summer flows for use in the phytoplankton node.
Seasonality factor	Range 0-1	A factor determining the ratio of summer potential TN concentration to mean annual potential TN concentration. Obtained from Tool 1 using dilution modelling (Plew et al. 2018; Whitehead et al. 2019).
Estuary type	type	ETI typology estuary type (Hume 2018). Obtained from Tool 1.
Sediment Load	g/m ² /d	The areal loading of sediment to estuaries. Obtained from Tool 1 and derived from sediment load model (Hicks et al. 2019).
Closure duration	always open, short close, long close	short close = days, long close = weeks to months. Decided by user.
Stratification	No / yes	Whether summer stratification is likely in the system. Decided by user.
Macroalgae	OMBT (Opportunistic Macroalgal Blooming Tool) EQR	Uses OMBT EQR derivation (WFD-UKTAG 2014) in Robertson et al. (2016b), seasonal worst case and calculated for whole estuary. Ranges from 0 to 1.
Phytoplankton	mg/m ³ chlorophyll	90th percentile summer monthly phytoplankton measures from representative areas of estuary water column (Borja et al. 2004; Plew et al. 2020b).
Sediment apparent Redox Potential Discontinuity	cm	Mean depth of apparent Sediment Redox Potential Discontinuity (aRPD), the depth of the boundary between oxic near-surface sediment and the underlying suboxic or anoxic sediment (Robertson et al. 2016b).
Mud	%	Mean percent mud (<63 µm particle diameter) in individual samples (Robertson et al. 2016b).
Sediment TOC	%	Mean of measured TOC (Total Organic Carbon) at 0-2cm depth; represents mean across estuary (Robertson et al. 2016b; Sutula et al. 2014).
Sediment trapping efficiency	Range 0-1	Mean proportion of the suspended sediment delivered to the estuary that deposits and remains there. Derived from sediment load model (Hicks et al. 2019).
Sediment deposition	mm/y	Mean rate of deposition of fine sediment in estuary. Derived from sediment load model (Hicks et al. 2019).
Oxygen depletion susceptibility	High/medium/low	Susceptibility of an estuary type to oxygen depletion in stratified or unstratified conditions.

Node	Unit	Definitions
Oxygen concentration	mg/L	Mean concentration of oxygen for summer conditions in stratified or unstratified conditions.
Macrobenthos	NZ AMBI	Represents mean across estuary (Robertson et al., 2015; Robertson et al., 2016).
Seagrass	% natural state	Percentage of estuary with >20% seagrass cover compared to Estimated Natural State Cover (ENSC) (Robertson et al. 2016b).
ETI primary score	Range 0-16	Maximum of primary indicator values.
ETI secondary score	Range 0-16	Mean of secondary indicator values.
Final ETI score	Range 0-1	Mean of maximum primary value and average of secondary indicator values, normalised between zero and 1 <i>cf</i> Tool 2 approach (Zeldis et al. 2017c).

Table 2-3: Background knowledge for the Conditional Probability Tables (CPTs) underpinning the BBN. Node linkages shown in Figure 2-1 are described in the indicated report sections using the methods, data sources and main references indicated. Note that the ‘standardised nodes’ in this table are not shown in Figure 2-1, but may be seen in Figure 4-1 to Figure 4-3.

Node linkages	Report section	Methods	Data sources	Main references
Salinity / Potential TN conc./ Macroalgae	3.1	Empirical/analytical model relationship	CLUES-estuary dilution modelling, Wriggle EQR database	Robertson et al. (2016b); Plew et al. (2018); Plew et al. (2020b)
Potential N conc. / Flushing / Seasonality / Salinity / Phytoplankton	3.2	Analytical model relationships	CLUES-Estuary dilution and phytoplankton modelling, hydrological modelling	Plew et al. (2018); (Plew et al. 2020b); Borja et al. (2004); Whitehead et al. (2019); Booker and Woods (2014)
Percent intertidal/ETI primary score	3.3	Analytical model/Empirical relationship	CLUES-Estuary dilution modelling, literature values for macroalgal and phytoplankton tolerances	Plew et al. (2018); Plew et al. (2020b)
Macroalgae / Sed. RPD	3.8	Empirical relationship	Wriggle EQR database, California estuaries	Sutula et al. (2014); Green et al. (2014)
Estuary type / Closure duration / Sed. trapping efficiency	3.4	Analytical Model relationships	NZ Coastal Hydrosystem Typology, Sediment Load Model,	Hume (2018); Hicks et al. (2019); Hume et al. (2007)
Sediment load / Sed. trapping efficiency / Sed. Deposition	3.5	Analytical Model relationships	Sediment Load Model / Wriggle mud database	Hicks et al. (2019); Robertson et al. (2015)
Sed. deposition / Mud	3.6	Empirical relationship	East coast USA estuaries	Townsend and Lohrer (2015)
Macroalgae / Mud / TOC	3.7	Empirical relationship	Wriggle/ES database / California estuaries	Robertson et al. (2016b); Sutula et al. (2014); Pelletier et al. (2011)
Macroalgae / TOC / sediment apparent redox potential discontinuity	3.8	Empirical relationship/Analytical Model relationships	California estuaries / Wriggle EQR database	Sutula et al. (2014); Green et al. (2014); Plew et al. (2020b)
Macroalgae / Mud / TOC / Macrobenthos	3.9	Empirical relationship	Wriggle TOC/Mud/Macrobenthos database	Robertson et al. (2016c); Green et al. (2014)
Stratification / Estuary type / Flushing / Phytoplankton / Oxygen	3.10	Empirical relationship/Analytical model relationship	Unpublished NIWA mooring data /mass balance modelling	Plew et al. (2020b); Salt ecology database; NIWA Coasts and Oceans database.
Potential TN conc. / Mud / Seagrass	3.11	Literature values	NZ, US field results	Robertson et al. (2016b); Matheson and Wadhwa (2012); Burkholder et al. (1994)
Indicator nodes / Standardised nodes	3.12	Calculated	Internal to BBN	None
Standardised primary nodes / ETI primary score	3.13	Calculated	Internal to BBN	Robertson et al. (2016b)
Standardised secondary nodes / ETI secondary score	3.14	Calculated	Internal to BBN	Robertson et al. (2016b)
ETI primary score and ETI secondary score / ETI final score	3.15	Calculated	Internal to BBN	Robertson et al. (2016b)

3 Descriptions and derivations of conditional probability tables (CPTs)

3.1 Salinity / potential total N concentration / macroalgal EQR

Plew et al. (2018) used simple dilution models to estimate potential total nitrogen (TN), nitrate (NO_3), total phosphorus (TP) and dissolved inorganic phosphorus (DRP) concentrations in, and flushing times of, estuaries and coastal water bodies across NZ. Potential concentrations are defined as the concentrations that would occur in the absence of uptake by algae, or losses or gains due to non-conservative processes such as denitrification (Plew et al. 2018). This modelling was used to predict potential total nitrogen (TN) concentrations for the estuaries of interest. These concentrations were regressed against a database of macroalgal Ecological Quality Rating (EQR) for 22 NZ estuaries, compiled by Wriggle Coastal Management (Robertson et al. 2016b; Zeldis et al. 2017c), derived using the Opportunistic Macroalgal Blooming Tool (OMBT) (WFD-UKTAG 2014). Plew et al. (2020b) derived an empirical relationship between EQR and potential TN concentration (Figure 3-1) from this dataset, that allowed prediction of macroalgal EQR from potential TN concentrations.

The regression was used to predict EQR at levels corresponding to thresholds of 0.8, 0.6 and 0.4, which are the thresholds between A-B (minimal-moderate), B-C (moderate-high) and C-D (high-very high) bands of macroalgal eutrophication derived for NZ estuarine health (Plew et al. 2020b; Robertson et al. 2016b). Observed annual TN loads and annual mean flows were used to calculate potential TN concentrations, while EQR observations were from peak growth (summer) periods. Our bandings therefore relate annual loads and flows to summer macroalgal response, which is typically when eutrophic growths are maximal.

This macroalgal modelling assumed that nitrogen (N) was the limiting nutrient and hence the BBN only models potential N and not potential phosphorus (P). Macroalgae are unlikely to show P limitation for N:P molar ratios less than 30:1 (Atkinson and Smith 1983). Plew et al. (2020b), in their assessment of estuary susceptibility to macroalgal eutrophication, showed that this condition was met for 95% of estuaries in the ETI dataset. Of the nine macroalgal-susceptible estuaries for which $\text{N/P} > 30:1$, 7 had a D band for susceptibility and the other two were C band. For the estuaries with $\text{N/P} > 30:1$, Plew et al. (2020b) assessed whether P limitation would be likely to result in a lower susceptibility band by reducing the potential N concentration to give an N/P molar ratio of 30:1, then obtaining the macroalgal susceptibility band from this modified potential N concentration. When this was done, the susceptibility bands remained the same for all the estuaries, showing that neglecting P had little effect on macroalgal susceptibility predictions because they had N and P so high that neither limited growth. It is valid, therefore, to assume that N is nearly always the limiting nutrient for macroalgae growth, a conclusion is supported by experimental assays in NZ estuaries (Barr 2007; Robertson and Savage 2018).

The assumption that macroalgae are seldom limited by P, is further supported by measurements of algal tissue N and P that have found that macroalgae can accumulate N well above the Redfield ratio of N:P = 16:1, with values in excess of 60:1 reported (Atkinson and Smith 1983; Fong et al. 1994). Recent NZ experiments show that P saturation concentration for *Gracilaria* (the concentration at which further increases in P have no effect on growth rates) is much lower than that for nitrogen (B. Dudley, NIWA, pers. comm.). This means that macroalgae can extract P from the water column even when P concentrations are low and that high tissue N:P ratios indicate that they continue to take up N even when the relative availability of P is low. Thus, it is appropriate to develop bandings based on N (Plew et al. 2020a).

To construct the CPT, the 95% EQR prediction intervals around this regression were used to allocate probabilities for each EQR state (Table 3-1) by fitting normal error distributions at each potential TN state. The more finely resolved states of potential TN at lower concentrations than higher concentrations (Figure 3-1) reflected the need to distinguish TN at lower levels where macroalgal growth changes rapidly with concentration (B. Dudley NIWA, pers. comm.; N. Barr, NIWA, pers. comm.).

Because estuarine macroalgal growth is inhibited by low salinity conditions (Martins et al. 1999), in the CPT we apply a high macroalgal EQR band (i.e., low macroalgal biomass) if the estuary salinity (calculated from the dilution modelling) is less than 5 psu, irrespective of potential TN concentrations. These are predominately in the A band, becoming increasingly in the B band with increasing potential TN. To accommodate high salinities (>30-36 psu which are used in the Phytoplankton CPT), salinities >30 psu are included in the macroalgae table. The associated probabilities of EQR state are the same as those between 5 and 30 psu (Table 3-1).

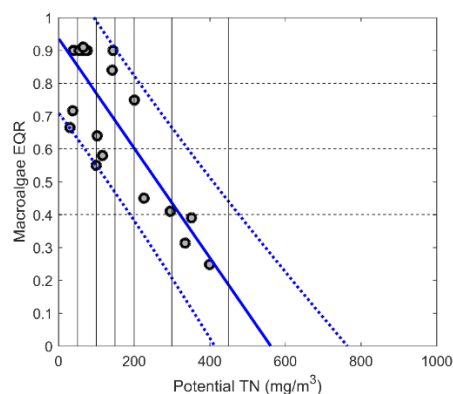


Figure 3-1: Observations of macroalgae Ecological Quality Rating (EQR) plotted against potential total nitrogen (TN) concentrations for 21 NZ estuaries. Data from Robertson et al. (2016b), Plew et al. (2018) and Plew et al. (2020b). Horizontal dotted lines demark Ecological Quality Rating (EQR) bands for macroalgae. Also shown are 95% prediction intervals used for calculating proportion of observations in each EQR band at various potential TN levels (vertical lines).

Table 3-1: Predicted effects of salinity and potential total nitrogen (TN) concentration on macroalgal Ecological Quality Rating (EQR) in NZ estuaries. EQR state % probabilities at each potential TN state were calculated by fitting Gaussian normal probability curves to the prediction interval of the linear regression of Figure 3-1.

Parent node states		State % probabilities: Macroalgal EQR			
Salinity	Potential TN conc.	0.8 to 1	0.6 to <0.8	0.4 to <0.6	0 to <0.4
0 to 5	0 to 50	97	3	0	0
0 to 5	50 to 100	89	11	0	0
0 to 5	100 to 150	81	19	0	0
0 to 5	150 to 200	73	27	0	0
0 to 5	200 to 300	65	35	0	0
0 to 5	300 to 450	54	45	1	0
0 to 5	450 to 5000	29	63	8	0
≥5 to 30	0 to 50	64	23	10	3
≥5 to 30	50 to 100	52	27	15	6
≥5 to 30	100 to 150	39	30	21	10
≥5 to 30	150 to 200	28	29	26	17
≥5 to 30	200 to 300	15	23	29	33
≥5 to 30	300 to 450	5	12	22	61
≥5 to 30	450 to 5000	0	1	2	97
≥30 to 35	0 to 50	64	23	10	3
≥30 to 35	50 to 100	52	27	15	6
≥30 to 35	100 to 150	39	30	21	10
≥30 to 35	150 to 200	28	29	26	17
≥30 to 35	200 to 300	15	23	29	33
≥30 to 35	300 to 450	5	12	22	61
≥30 to 35	450 to 5000	0	1	2	97

3.2 Potential TN concentration / flushing / salinity / phytoplankton

Plew et al. (2020b) detailed the derivation, validation and performance of an analytical model for predicting phytoplankton concentrations in NZ estuaries using a dilution modelling approach. In brief, the rate of change of phytoplankton in the estuary was balanced between growth rate and advection. This method accounts for phytoplankton concentration in the coastal region, the freshwater inflow, the tidal period, the tidal prism, the estuary volume at high tide, return flows and incomplete mixing, and the dynamics of N and P concentrations and their kinetics of algal growth.

In the BBN it is assumed that P is not limiting for phytoplankton growth and hence uses only N in its modelling. This is supported by the finding by Plew et al. (2020b) that 81% of the estuaries in the ETI Tool 1 dataset were limited by N, for estuaries susceptible to phytoplankton eutrophication. This result was supported by overseas findings of dominant N limitation of estuarine phytoplankton (NRC 2000).

The bandings applied to responses of modelled phytoplankton to potential TN (Figure 3-2) shows the interaction of salinity, nutrient concentration, flushing time and phytoplankton concentration. Some coastal systems are freshwater (e.g., coastal lakes, so not strictly “estuarine”) or have low salinities

that would suppress estuarine phytoplankton growth. For those freshwater or brackish, oligohaline (salinity < 5 psu) systems, we applied bandings from the New Zealand National Policy Statement for Freshwater Management for the maximum chl-*a* concentrations in lakes (Ministry for the Environment 2018). For mesohaline/polyhaline (salinity 5-30 psu) systems and euhaline (salinity >30 psu) systems, the Basque estuary thresholds (Borja et al. 2004; Robertson et al. 2016b) were used for banding. The Basque estuary bandings were developed for the 90th percentile of monthly observations but applied to the model using mean annual flows and annual N loads.

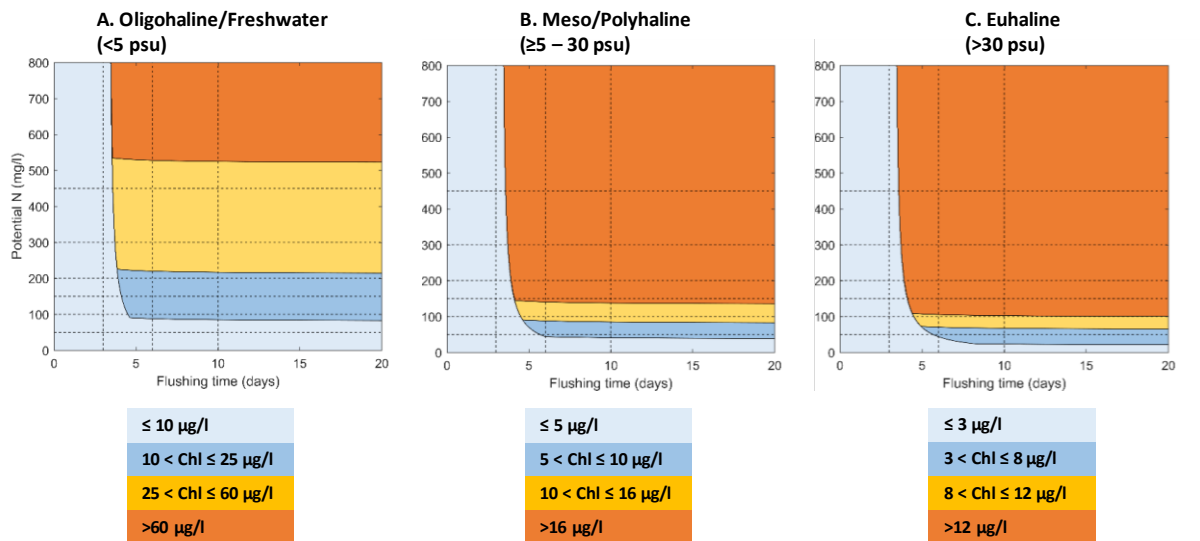


Figure 3-2: Contours of predicted chlorophyll-*a* (chl-*a*) concentrations (µg/l) as a function of the potential total nitrogen concentration and estuary flushing time. The models show chl-*a* concentrations when phosphorus is not limiting and assumes a specific growth rate $k = 0.3 \text{ d}^{-1}$ and a half saturation coefficient for growth response to nitrogen of 35 mg m^{-3} . Colour bands show ecological responses for (A) oligohaline/freshwater systems, (B) meso/polyhaline, and (C) euhaline systems, to chl-*a* levels from minimal to moderate, high and very high levels of eutrophication. Vertical and horizontal lines denote regions for which probabilities are calculated in the CPT (Table 3-2).

The models were used to predict phytoplankton concentration state at each salinity, flushing and potential TN state (Plew et al. 2020b).

The states of potential TN used were the same as for macroalgae, and were finely resolved at low concentrations, again reflecting the need to distinguish TN at lower levels where phytoplankton growth changes rapidly with concentration (Eppley 1969). Flushing time states were chosen to range from those below which no blooms form (<3 d) to those above which chlorophyll levels are determined solely by nutrient concentration (> 6 d) (Figure 3-2). Intermediate levels were chosen (4 and 6 d) to be spread between the minimum and maximum flushing rates. The dependence of phytoplankton response on differing system salinities is accounted for by the ‘Phytoplankton standardised’ node (Table 3-3) that maps the ‘Phytoplankton’ node to the ‘ETI primary’ node (see section 3.12 for further details regarding ‘Standardised’ nodes). That CPT accounts for the higher bandings for oligohaline (< 5 psu) than mesohaline/polyhaline or euhaline ≥5->30 psu) systems.

The detrimental effects of phytoplankton blooms (particularly deoxygenation of the lower water column) are more common in summer when water column stratification is more likely (see Oxygen node section 3.10 for further description). To capture this seasonality, it is more appropriate to use a summer flushing time and summer potential TN concentration when predicting phytoplankton than

mean annual values. This was achieved using a ratio of February (summer) flows to mean annual flow via statistical modelling of NZ river reaches (Booker and Woods 2014). Whitehead et al. (2019) predicted median nutrient concentrations in all River Environment Classification reaches for summer and winter. These, along with predicted mean and February flows, were used to calculate the summer and annual nutrient load and flow to each estuary in the Tool 1 database and from these, the flow-weighted summer nutrient concentration ratio was calculated. The dilution modelling of Plew et al. (2018) was then used to estimate estuary dilution factors from the February mean flow and February coastal nitrate concentrations extracted from the oceanic nutrient climatology used in the modelling. The summer freshwater inflow TN concentration, summer dilution factor and summer oceanic N concentrations were used to estimate the summer potential TN in each estuary.

Frequency distributions of the ratios of summer and winter estuary potential TN concentrations had a median of 0.56, with the central third of the ratios between 0.504 and 0.647. On this basis, the seasonality factor evaluating the ratio of mean annual to summer estuary potential TN was set with bands as <0.5, 0.5 to 0.65, >0.65.

To construct the CPT evaluating relationships of seasonality, flushing and potential TN to phytoplankton (Table 3-2), the seasonality factor distribution was split into three (at 33% and 67%), and the seasonality at the mid-point of each (at percentiles of 16.7%, 50% and 83.3%) used to adjust annual potential TN concentrations. The corresponding seasonality factors were 0.453, 0.558, and 0.780. The chl-*a* concentrations in the table were calculated across the range of potential TN and flushing times values within each TN and flushing time bands, with the potential TN values scaled by the seasonality factors.

The scores for phytoplankton responses (in terms of primary indicator score) in oligohaline (0 to 5 psu), meso/polyhaline (5 to 30 psu) and euhaline (30 to 36 psu) estuaries were then predicted using the salinity driver node and the phytoplankton node (Figure 2-1 and Table 3-3).

Table 3-2: Predicted effects of seasonality factor, estuary flushing time (d) and potential TN concentration (mg/m³) on phytoplankton concentrations (mg/m³) in NZ estuaries.

Parent Node states			State % probabilities: Phytoplankton					
Seasonality factor	Flushing time	Nutrients	0-5	>5-10	>10-15	>15-25	>25-60	>60
<0.5	0-3	0-50	100	0	0	0	0	0
<0.5	0-3	>50-100	100	0	0	0	0	0
<0.5	0-3	>100-150	100	0	0	0	0	0
<0.5	0-3	>150-200	100	0	0	0	0	0
<0.5	0-3	>200-300	100	0	0	0	0	0
<0.5	0-3	>300-450	100	0	0	0	0	0
<0.5	0-3	>450	100	0	0	0	0	0
<0.5	>3-6	0-50	100	0	0	0	0	0
<0.5	>3-6	>50-100	100	0	0	0	0	0
<0.5	>3-6	>100-150	81	19	0	0	0	0
<0.5	>3-6	>150-200	61	36	3	0	0	0
<0.5	>3-6	>200-300	46	0	51	3	0	0
<0.5	>3-6	>300-450	35	0	0	65	0	0
<0.5	>3-6	>450	24	0	0	5	71	0

Parent Node states			State % probabilities: Phytoplankton					
Seasonality factor	Flushing time	Nutrients	0-5	>5-10	>10-15	>15-25	>25-60	>60
<0.5	>6-10	0-50	100	0	0	0	0	0
<0.5	>6-10	>50-100	86	14	0	0	0	0
<0.5	>6-10	>100-150	0	100	0	0	0	0
<0.5	>6-10	>150-200	0	81	19	0	0	0
<0.5	>6-10	>200-300	0	0	87	13	0	0
<0.5	>6-10	>300-450	0	0	0	100	0	0
<0.5	>6-10	>450	0	0	0	6	94	0
<0.5	>10	0-50	100	0	0	0	0	0
<0.5	>10	>50-100	75	25	0	0	0	0
<0.5	>10	>100-150	0	100	0	0	0	0
<0.5	>10	>150-200	0	69	31	0	0	0
<0.5	>10	>200-300	0	0	82	18	0	0
<0.5	>10	>300-450	0	0	0	100	0	0
<0.5	>10	>450	0	0	0	5	95	0
0.5-0.65	0-3	0-50	100	0	0	0	0	0
0.5-0.65	0-3	>50-100	100	0	0	0	0	0
0.5-0.65	0-3	>100-150	100	0	0	0	0	0
0.5-0.65	0-3	>150-200	100	0	0	0	0	0
0.5-0.65	0-3	>200-300	100	0	0	0	0	0
0.5-0.65	0-3	>300-450	100	0	0	0	0	0
0.5-0.65	0-3	>450	100	0	0	0	0	0
0.5-0.65	>3-6	0-50	100	0	0	0	0	0
0.5-0.65	>3-6	>50-100	96	4	0	0	0	0
0.5-0.65	>3-6	>100-150	68	32	0	0	0	0
0.5-0.65	>3-6	>150-200	52	9	40	0	0	0
0.5-0.65	>3-6	>200-300	40	0	23	38	0	0
0.5-0.65	>3-6	>300-450	30	0	0	45	25	0
0.5-0.65	>3-6	>450	22	0	0	0	71	7
0.5-0.65	>6-10	0-50	100	0	0	0	0	0
0.5-0.65	>6-10	>50-100	51	49	0	0	0	0
0.5-0.65	>6-10	>100-150	0	100	0	0	0	0
0.5-0.65	>6-10	>150-200	0	9	91	0	0	0
0.5-0.65	>6-10	>200-300	0	0	33	67	0	0
0.5-0.65	>6-10	>300-450	0	0	0	61	39	0
0.5-0.65	>6-10	>450	0	0	0	0	90	10
0.5-0.65	>10	0-50	100	0	0	0	0	0
0.5-0.65	>10	>50-100	42	58	0	0	0	0
0.5-0.65	>10	>100-150	0	99	1	0	0	0
0.5-0.65	>10	>150-200	0	1	99	0	0	0
0.5-0.65	>10	>200-300	0	0	29	71	0	0
0.5-0.65	>10	>300-450	0	0	0	58	42	0
0.5-0.65	>10	>450	0	0	0	0	89	11
>0.65	0-3	0-50	100	0	0	0	0	0
>0.65	0-3	>50-100	100	0	0	0	0	0

Parent Node states			State % probabilities: Phytoplankton					
Seasonality factor	Flushing time	Nutrients	0-5	>5-10	>10-15	>15-25	>25-60	>60
>0.65	0-3	>100-150	100	0	0	0	0	0
>0.65	0-3	>150-200	100	0	0	0	0	0
>0.65	0-3	>200-300	100	0	0	0	0	0
>0.65	0-3	>300-450	100	0	0	0	0	0
>0.65	0-3	>450	100	0	0	0	0	0
>0.65	>3-6	0-50	100	0	0	0	0	0
>0.65	>3-6	>50-100	80	20	0	0	0	0
>0.65	>3-6	>100-150	52	12	36	0	0	0
>0.65	>3-6	>150-200	40	0	25	35	0	0
>0.65	>3-6	>200-300	32	0	0	58	11	0
>0.65	>3-6	>300-450	25	0	0	0	75	0
>0.65	>3-6	>450	19	0	0	0	33	48
>0.65	>6-10	0-50	100	0	0	0	0	0
>0.65	>6-10	>50-100	8	92	0	0	0	0
>0.65	>6-10	>100-150	0	21	79	0	0	0
>0.65	>6-10	>150-200	0	0	34	66	0	0
>0.65	>6-10	>200-300	0	0	0	80	20	0
>0.65	>6-10	>300-450	0	0	0	0	100	0
>0.65	>6-10	>450	0	0	0	0	41	59
>0.65	>10	0-50	100	0	0	0	0	0
>0.65	>10	>50-100	2	98	0	0	0	0
>0.65	>10	>100-150	0	15	85	0	0	0
>0.65	>10	>150-200	0	0	28	72	0	0
>0.65	>10	>200-300	0	0	0	77	23	0
>0.65	>10	>300-450	0	0	0	0	100	0
>0.65	>10	>450	0	0	0	0	40	60

Table 3-3: Mapping of predicted phytoplankton concentrations (Table 3-2) to ETI Primary scores (0-16). Effects of salinity (psu) and phytoplankton concentrations (mg chl-*a*/m³) on phytoplankton standardised concentrations in NZ oligohaline (0 to 5 psu), meso/polyhaline (5 to 30 psu) and euhaline (30 to 36 psu) estuaries is shown.

Parent Node states:		State % probabilities: Phytoplankton standard			
Salinity	Phytoplankton	1 to 5	5 to 9	9 to 13	13 to 16
0 to 5	0 to 5	100	0	0	0
0 to 5	5 to 10	100	0	0	0
0 to 5	10 to 15	0	100	0	0
0 to 5	15 to 25	0	100	0	0
0 to 5	25 to 60	0	0	100	0
0 to 5	60 to 1000	0	0	0	100
5 to 30	0 to 5	100	0	0	0
5 to 30	5 to 10	0	100	0	0
5 to 30	10 to 15	0	0	100	0
5 to 30	15 to 25	0	0	10	90

Parent Node states:		State % probabilities: Phytoplankton standard			
Salinity	Phytoplankton	1 to 5	5 to 9	9 to 13	13 to 16
5 to 30	25 to 60	0	0	0	100
5 to 30	60 to 1000	0	0	0	100
30 to 36	0 to 5	60	40	0	0
30 to 36	5 to 10	0	60	40	0
30 to 36	10 to 15	0	0	40	60
30 to 36	15 to 25	0	0	0	100
30 to 36	25 to 60	0	0	0	100
30 to 36	60 to 1000	0	0	0	100

3.3 Percent intertidal/primary indicators score

In the BBN, there is a link between the driver node which evaluates the percentage of the estuary which is intertidal and the ETI primary score node (Figure 2-1). This is because the relative influence of phytoplankton and macroalgal eutrophication depends on estuary morphology. The main effects of phytoplankton eutrophication are oxygen depletion and high light attenuation in deeper and often stratified estuarine systems, which typically do not occur in New Zealand SDEs (lagoon estuaries) when they are permanently open (Robertson et al. 2016a). Phytoplankton effects are more likely in SSRTREs (river estuaries) and DSDEs (deep estuaries), particularly those with longer flushing times (Plew et al. 2020b). Using the ETI Tool 1 database, it has been found that the great majority of estuaries with intertidal areas less than 20% are SSRTREs, while the great majority of SDEs have intertidal areas greater than 40%. To prevent the phytoplankton primary indicator having effect when operating the BBN for estuaries with intertidal areas greater than 40% (i.e., for SDEs), the BBN selects the macroalgal primary indicator as the driver of the ETI primary score node. For estuaries with intertidal areas less than 5% the BBN selects the phytoplankton primary indicator as the driver of the ETI primary score node. If the intertidal area is between 5% and 40%, the BBN considers both macroalgal and phytoplankton indicators, and the ETI primary score node is scored using the worst of the macroalgae and phytoplankton indicators. The percent intertidal area CPT thus has three decision settings (0-5%, >5-<40% and >40%). The ETI primary score node CPT which incorporates these settings and maps them to the various combinations of standardised macroalgae and phytoplankton scores is very large and is not shown here. However, it may be examined by opening that node in Netica using the ETI Tool 3 application and opening the 'Table' tab.

Although the percent intertidal setting affects whether the ETI primary score node is driven by macroalgae or phytoplankton, it does not affect how the nutrient and flushing driver nodes affect the macroalgae and phytoplankton nodes (Figure 2-1). Therefore, if the estuary is a SDE, but is known to have areas that have deep holes with high nutrients and low flushing, the user may wish to consider the results of the phytoplankton node in decision-making. Conversely, if the estuary is an SSRTRE or DSDE, but is known to have small but important intertidal areas, the user may wish to consider results of the macroalgae node.

3.4 Estuary type / closure duration / sediment trapping efficiency

Along with autochthonous organic matter accumulation, estuary muddiness (accumulation of fine sediments) from allochthonous (predominately catchment) sources is also a major factor impacting estuary conditions. Elevated delivery and retention of terrigenous mud (<63 µm particle diameter) to estuaries can impair feeding, behavioural responses, larval recruitment, and trophic interactions in

coastal food-webs (Jones et al. 2011; Lohrer et al. 2004; Lohrer et al. 2006; Pratt et al. 2014; Robertson et al. 2015). These less permeable, muddy sediments often retain higher % organic matter (%TOC) and nutrients (Engelsen et al. 2008; Huettel and Rusch 2000) which, in turn, can drive eutrophication (Zeldis et al. 2020).

Catchment-derived muddiness arises from an interaction of the rate of fine sediment delivery (load) and efficiency of its trapping in the estuary. High trapping efficiency means that most of the fine sediment delivered from the catchment deposits in the estuary. A simple, zero-dimensional sediment mass balance model for estuary sediment trapping efficiency was developed by Hicks et al. (2019). The model balances the influx of sediment from rivers, deposition in the estuary, resuspension by waves, and entrainment by currents with export through the mouth to the ocean (Figure 3-3).

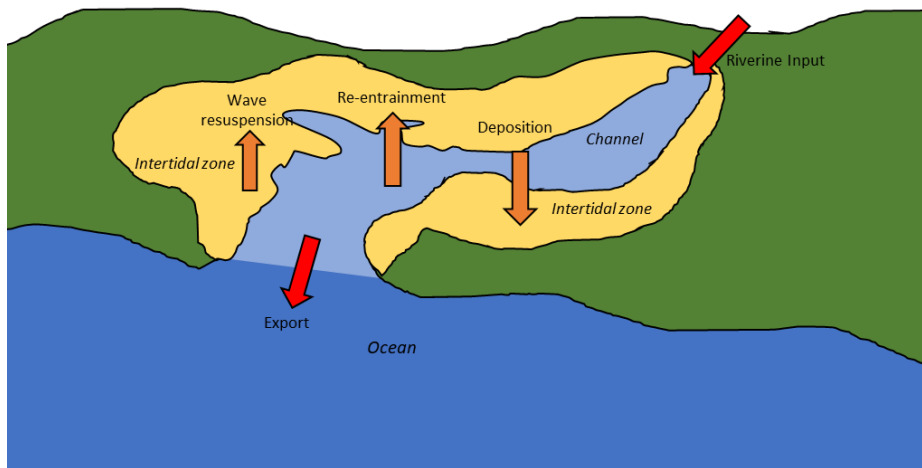


Figure 3-3: Conceptual diagram of an estuary showing the terms in the sediment mass balance model. Sediment is supplied via riverine input and exported to the sea through the mouth. A fraction deposits within the estuary. Resuspension by waves occurs on intertidal areas, and re-entrainment by currents occurs in tidal channels. The version of the model used in this work differs slightly from the form used by Hicks et al. (2019) in its treatment of wave resuspension.

The sediment mass balance model is described by the following equation:

$$S_{out} = S_{in} + E_w + E_c - D \quad (1)$$

where

S_{in} = sediment influx from the catchment (kg/s)¹

S_{out} = sediment export to the ocean (kg/s)

E_w = resuspension of sediment by waves (kg/s)

E_c = re-entrainment by currents (kg/s)

D = settling of sediment in the estuary (kg/s).

¹ The working sediment budget components were calculated with units of kg/s. The results, providing mean annual values, are reported with units of t/y.

Sediment trapping efficiency can be calculated as the fraction of incoming sediment that is retained within the estuary:

$$\eta = \frac{S_{in} - S_{out}}{S_{in}} \quad (2)$$

While all the terms in Equation (1) are time-varying, they occur over different time scales that are not necessarily coupled. For example, sediment influx is related to river inflow, re-entrainment is determined by both river inflow and tidal flow, and resuspension by waves is driven by wind. These data were not available for all estuaries in a manner that would allow true daily sediment budgets to be calculated. Instead, sediment influxes, settling, and export were calculated over a range of inflows from a modelled daily flow duration curve. A sediment rating curve was developed from the flow duration curve to account for higher sediment inflow concentrations during high flows. River and sediment inputs were treated as quasi-steady for each point on the flow duration curve, with tides superimposed to calculate re-entrainment. Re-entrainment was calculated from estimating bed shear stress distributions over tidal cycles at each inflow and applied over the estimated portion of the estuary of tidal channels. Entrainment was limited so that it did not exceed deposition (i.e., it stopped deposition occurring in subtidal areas but did not allow for erosion). Wave resuspension was calculated by determining the average portion of the estuary area where the bed shear stress exceeded the critical shear stress for sediment resuspension. This calculation was based on wind-velocity and direction frequency distributions and reach (dimensions of the estuary). Like entrainment, wave resuspension was assumed to balance deposition over the portion of the estuary where wave resuspension occurs (in the original model an annual average wave resuspension mass flux was calculated, capped at the annual riverine sediment input). Collectively, the wave resuspension and entrainment terms reduce the deposition of sediment.

The net rate of sediment accumulation in the estuary was calculated as the difference between the sediment input and export, i.e., $S_{in} - S_{out}$. This was averaged over all inflows to obtain the net average accumulation rate (t/y). To convert this to a deposition rate (mm/y), the net accumulation rate was divided by estuary area and deposited sediment bulk density ($\rho_b = 1500 \text{ kg/m}^3$).

This formulation of the trapping efficiency model does not allow for predictions of net erosion within an estuary. The implicit assumption is that only the fine sediments delivered each year are available for resuspension.

Trapping efficiencies were calculated for 399 NZ estuaries, using estuary properties found in the Coastal Explorer database (Hume et al. 2007). Estuaries were grouped by type, and frequency distributions of trapping efficiencies, assigned to bands of >0.95, 0.85-0.95, 0.5-0.85, 0.1-0.5, < 0.1 determined for each type (Table 3-4). Coastal lakes were not well defined, and in some cases, systems identified as coastal lakes were more riverine. The frequency distribution for coastal lakes was modified to increase trapping efficiencies, based on those systems being considered true coastal lakes. In general terms, coastal lakes have highest trapping efficiencies, followed by DSDE, then SIDES. SSRTRE's have low trapping efficiencies.

The trapping efficiency calculations were run assuming all estuaries empty to the sea. Some estuaries are ICOEs and can have short (days) or long (weeks to months) closures. These closures are likely to increase trapping efficiencies, although they generally open during high flow periods, and large portions of sediment loads are delivered during high flows. Consequently, it is likely that on an

annual basis, trapping efficiencies increase only by small amounts due to intermittent mouth closures.

Coastal lakes are, by definition, usually closed, and DSDEs are large systems that will not experience mouth closures. Therefore, we only considered closure states for SIDs and SSRTREs. For these systems, we approximated the effect of short closures by assuming that 5% more sediment is trapped, and 30% more for long closures (a 30% increase would result in a trapping efficiency of 0.5 increasing to $(1-0.7*(1-0.5)) = 0.65$, while a trapping efficiency of 0.8 increases to $1-0.7*(1-0.8) = 0.86$). Frequency distributions for the short and long closure states were calculated from these modified trapping efficiencies (Table 3-5).

The final probability estimates of trapping efficiency accounting for estuary type and closure state (Table 3-6) were estimated by cross-multiplying the results of Table 3-4 and Table 3-5.

Table 3-4: Frequency distributions of trapping efficiency for each ETI estuary type, in their open state.

Trapping efficiency	DSDE	SIDE	SSRTRE	Coastal Lake
0.95-1.0	77%	33%	0%	92%
0.85-0.95	15%	40%	1%	5%
0.5-0.85	7%	20%	10%	2%
0.1-0.5	1%	4%	28%	1%
0-0.1	0%	3%	61%	0%

Table 3-5: Trapping efficiencies for SIDE and SSRTRE with short and long closure.

Trapping efficiency	SIDE	SIDE	SSRTRE	SSRTRE
	Short closure	Long closures	Short closure	Long closure
0.95-1.0	33%	41%	0%	1%
0.85-0.95	41%	39%	2%	3%
0.5-0.85	18%	15%	13%	19%
0.1-0.5	4%	5%	30%	76%
0 - 0.1	3%	0%	55%	1%

Table 3-6: Predicted effects of estuary type and estuary closure state on estuary sediment trapping efficiency.

Parent node state		State % probabilities: trapping efficiency				
Estuary Type	Closure duration	0 to 0.1	0.1-0.5	0.5-0.85	0.85-0.95	0.95 to 1.0
Coastal Lake	Open	0	1	2	5	92
Coastal Lake	Short Closure	0	1	2	5	92
Coastal Lake	Long Closure	0	1	2	5	92
DSDE	Open	0	1	7	15	77
DSDE	Short Closure	0	1	7	15	77
DSDE	Long Closure	0	1	7	15	77
SIDE	Open	3	4	20	40	33
SIDE	Short Closure	4	4	18	41	33
SIDE	Long Closure	0	5	15	39	41
SSRTRE	Open	61	28	10	1	0
SSRTRE	Short Closure	55	30	13	2	0
SSRTRE	Long Closure	1	76	19	3	1

3.5 Sediment load / sediment trapping efficiency / sediment deposition

Annual deposition rates (mm/y) are determined from sediment load (L , g/m²/d) and trapping efficiency, assuming a sediment bulk density of 1500 kg/m³.

$$d = \frac{365\eta L}{1500} \quad (3)$$

For the BBN, sediment load bands were defined, and a probability distribution table generated by calculating the distribution of deposition rates that can occur within each combination of sediment load band and trapping efficiency band. These deposition rate distributions were divided into five bands from low to high (<0.1 mm/y, 0.1-0.5 mm/y, 0.5-2mm/y, 2-5 mm/y, >5 mm/y) to derive the CPT linking trapping efficiency bands and load bands to deposition rate (Table 3-7).

The choice of deposition rate bands is informed by the ANZECC default guideline value of 2 mm/y of sediment accumulation above the natural annual sedimentation rate (Townsend and Lohrer 2015), noting that natural sediment rates are seldom known (see section 3.6, below).

Table 3-7: Predicted effects of estuary sediment trapping efficiency and sediment load on estuary sediment deposition rate.

Parent node state		State % probabilities: Deposition Rate (mm/y)						
Trapping efficiency	Sed. load (g/m ² /d)	0 to 0.1	0.1 to 0.5	0.5 to 1	1.0 to 2	2 to 5	5 to 10	10 to 20
0-0.1	0-1	100	0	0	0	0	0	0
0-0.1	1-5	98	2	0	0	0	0	0
0-0.1	5-10	59	41	0	0	0	0	0
0-0.1	10-20	29	71	0	0	0	0	0
0-0.1	20-50	13	54	30	3	0	0	0
0-0.1	50-100	6	24	30	37	3	0	0
0-0.1	100-1000	1	4	5	10	18	13	49
0.1-0.5	0-1	98	2	0	0	0	0	0
0.1-0.5	1-5	27	70	3	0	0	0	0
0.1-0.5	5-10	0	48	47	5	0	0	0
0.1-0.5	10-20	0	11	37	47	5	0	0
0.1-0.5	20-50	0	0	9	33	54	4	0
0.1-0.5	50-100	0	0	0	5	43	47	5
0.1-0.5	100-1000	0	0	0	0	3	9	88
0.5-0.85	0-1	76	24	0	0	0	0	0
0.5-0.85	1-5	0	68	31	1	0	0	0
0.5-0.85	5-10	0	0	32	67	1	0	0
0.5-0.85	10-20	0	0	0	32	68	0	0
0.5-0.85	20-50	0	0	0	0	47	52	1
0.5-0.85	50-100	0	0	0	0	0	32	68
0.5-0.85	100-1000	0	0	0	0	0	0	100
0.85-0.95	0-1	64	36	0	0	0	0	0
0.85-0.95	1-5	0	50	40	10	0	0	0
0.85-0.95	5-10	0	0	0	84	16	0	0
0.85-0.95	10-20	0	0	0	0	100	0	0
0.85-0.95	20-50	0	0	0	0	17	69	14
0.85-0.95	50-100	0	0	0	0	0	0	100
0.85-0.95	100-1000	0	0	0	0	0	0	100
0.95-1.0	0-1	60	40	0	0	0	0	0
0.95-1.0	1-5	0	50	37	13	0	0	0
0.95-1.0	5-10	0	0	0	72	28	0	0
0.95-1.0	10-20	0	0	0	0	100	0	0
0.95-1.0	20-50	0	0	0	0	10	70	20
0.95-1.0	50-100	0	0	0	0	0	0	100
0.95-1.0	100-1000	0	0	0	0	0	0	100

3.6 Sediment deposition / mud

The BBN %mud node is driven by sediment deposition rate. Thresholds for %mud of 12%, 25% and 34% (mean for an estuary) were selected based on Robertson et al. (2016c) who showed these were important thresholds for macrobenthic health (see section 3.9). We assumed that the ANZECC sedimentation default guideline (Townsend and Lohrer 2015) value of 2 mm/y above the natural

annual sedimentation rate causes detrimental effects similar to those at a 34% mud content (associated with ‘transitional to pollution’ in terms of macrobenthic health AMBI index (Robertson et al. 2016c)². We thus equated a deposition of >2 mm/y with a mud content of >34%. Based on this approximation, a CPT linking fine sediment deposition rate to %mud was created (Table 3-8).

Table 3-8: Predicted effects of estuary sediment deposition on estuary %mud.

Parent node state Deposition rate (mm/y)	State % probabilities: %mud			
	0 to 12	12 to 25	25 to 34	34 to 100
0 to 0.1	90	9	1	0
0.5 to 1	9	80	9	2
1 to 2	2	9	80	9
2 to 5	1	5	20	74
5 to 10	0	1	19	80
10 to 20	0	1	1	98

3.7 Macroalgae / mud / sediment TOC

Estuarine sediments with high organic matter content are often associated with chronic macroalgal blooms which, upon decomposition, contribute locally-produced (autochthonous) organic matter to sediments (Sutula et al. 2014). The rate of autochthonous organic matter production and its microbial respiration are key elements of the estuarine eutrophication problem (Robertson et al. 2016b; Sutula et al. 2014), associated with adverse sedimentary environmental conditions including depleted oxygen and excessive ammonium and hydrogen sulphide concentrations (Gray et al. 2002; Hyland et al. 2005; Robertson et al. 2015; Robertson et al. 2016c).

Sutula et al. (2014) derived relationships between macroalgal biomass (dw macroalgae/m²) and measures of sediment total organic carbon (%TOC) measured at 16 sites in eight California estuaries. We combined this with the macroalgal dw to EQR conversions (see section 3.8), to predict %TOC state probabilities for the four EQR parent node states (Table 3-9).

The four levels of %TOC state probabilities corresponding to EQR Band A (0 to 0.5% TOC) to Band D (>2% TOC) in Table 3-9 were estimated as follows. When relating apparent Redox Potential Discontinuity (aRPD) to %TOC (see section 3.8), Sutula et al. (2014) showed a ‘step’ threshold of aRPD at < 0.5 %TOC, below which the effect of macroalgae on aRPD was at a ‘reference’ (low impact) level. Robertson et al. (2016b) (their Table 8), associated this level of %TOC with low impact (Band A) which we associate with high macroalgal EQR (Table 3-9). At the other end of the scale, Sutula et al. (2014) showed a ‘slope’ threshold of 1.1 %TOC, where ‘exhaustion’ levels of impact on aRPD were first detected. We modified this to align with Robertson et al. (2016c) who showed a significant macrofaunal disturbance threshold at %TOC ≥ 1.2% (see section 3.9, below). We associate this with low macroalgal EQR in Table 3-9.

The %TOC probabilities of Table 3-9 were therefore distributed between %TOC levels expected to elicit effects ranging between ‘reference’ and ‘exhaustion’ levels of impact. Intermediate probabilities were allocated accounting for the relationships between macroalgal biomass and TOC

² AMBI (AZTI Marine Benthic Index) Ecological Groups were defined in terms of component fauna and their mud tolerances in Robertson et al. (2015).

shown in Figure 6 of Sutula et al. (2014), where high %TOC occurs at high macroalgal biomass (low EQR), and a lower %TOC occurs at low biomass (high EQR).

Table 3-9: Predicted effects of macroalgal EQR on %TOC.

Parent node state Macroalgal EQR	State % probabilities: %TOC			
	0 to 0.5	0.5 to 1.2	1.2 to 2	2 to 10
0.8 to 1	60	30	9	1
0.6 to <0.8	30	40	20	10
0.4 to <0.6	10	30	40	20
0 to <0.4	5	5	10	80

Sediment %TOC levels also vary predictably with degree of muddiness in sediments, as shown by Pelletier et al. (2011) who developed a relationship between square root (sediment %TOC) and %Mud using 446 reference sites in eastern USA estuaries:

$$\sqrt{\%TOC} = 0.018 \times \%mud + 0.34.$$

Here, we used mean %mud and %TOC data from individual samples in five Southland estuaries (New River, Jacobs River, Haldane, Fortrose and Freshwater estuaries: data provided by Wriggle Environmental Consultants) to derive this relationship (Figure 3-4). The resulting fit:

$$\sqrt{\%TOC} = 0.017 \times \%mud + 0.38,$$

($R^2 = 0.78$) was close to that obtained by Pelletier et al. (2011), derived from their much larger dataset. The Southland relationship was used to derive a CPT relating %Mud to %TOC distribution using the error structure in the relationship of Figure 3-4 (Table 3-10).

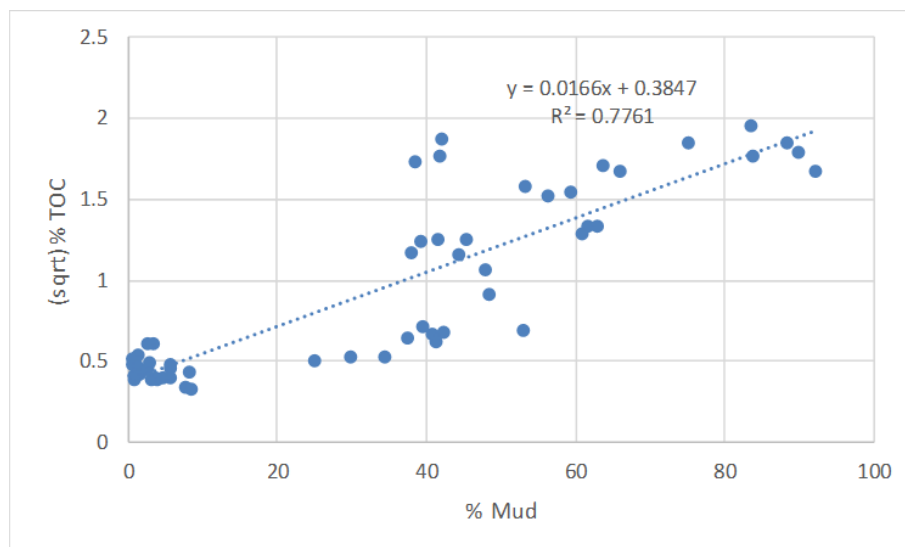


Figure 3-4: Relationship of %mud and %TOC in five Southland SIDE and SSRTRE estuaries. Data were fitted following methods of Pelletier et al. (2011).

The states of %TOC and %mud in Table 3-10 are those used in the macrobenthic node (Section 3.9) to predict macrofaunal health (along with macroalgae).

Table 3-10: Predicted effects of %mud on %TOC.

Parent node state % Mud	State % probabilities: %TOC			
	0 to 0.5	0.5 to 1.2	1.2 to 2	2 to 10
0 to 12	79	20	1	0
12 to 25	52	41	6	0
25 to 34	26	53	18	2
34 to 100	2	15	25	57

The final macroalgae / mud / %TOC CPT (Table 3-11) was derived by cross-multiplying Table 3-9 and Table 3-10.

Table 3-11: Predicted effects of macroalgal EQR and %mud on %TOC.

Parent node state		State % probabilities % TOC			
Macroalgal EQR	% Mud	0 to 0.5	0.5 to 1.2	1.2 to 2	2 to 10
0.8 to 1	0 to 12	88	11	0	0
0.8 to 1	12 to 25	74	25	1	0
0.8 to 1	25 to 34	55	42	3	0
0.8 to 1	34 to 100	77	20	2	0
0.6 to <0.8	0 to 12	71	28	1	0
0.6 to <0.8	12 to 25	47	49	4	0
0.6 to <0.8	25 to 34	26	61	13	0
0.6 to <0.8	34 to 100	47	37	11	5
0.4 to <0.6	0 to 12	47	48	5	0
0.4 to <0.6	12 to 25	24	64	11	1
0.4 to <0.6	25 to 34	10	61	28	2
0.4 to <0.6	34 to 100	17	35	24	23
0 to <0.4	0 to 12	16	52	25	6
0 to <0.4	12 to 25	4	35	28	33
0 to <0.4	25 to 34	1	18	38	44
0 to <0.4	34 to 100	0	2	5	93

3.8 Macroalgae / TOC / sediment apparent Redox Potential Discontinuity

As an indicator of estuary ecosystem condition, a shallow apparent Redox Potential Discontinuity (aRPD) depth (the depth that marks the boundary between oxic near-surface sediment and the underlying suboxic or anoxic sediment) has been related to reduced benthic habitat and quality for fauna and alteration in estuary community structure (Green et al. 2014; Sutula et al. 2014). Sutula et al. (2014) used sediment profile imagery at 16 sites across eight California estuaries, to identify thresholds of adverse effects of macroalgal biomass, sediment organic carbon (% OC) and sediment nitrogen (% N) concentrations on aRPD. They showed that aRPD decreased as TOC increased until a 'break point' beyond which further increases in TOC caused no further decrease in aRPD. They showed a linear relationship between aRPD and low values of TOC which, inferring from their Figure 5 (Figure 3-5), can be written as: $aRPD = 5.8 - 3.84 TOC$.

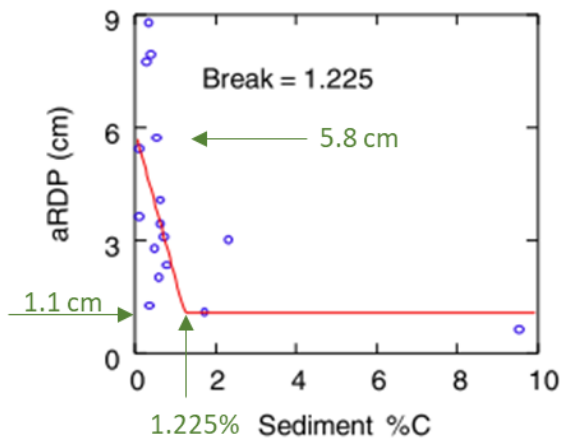


Figure 3-5: Sediment %TOC vs aRPD. From Sutula et al (2014): their Figure 5.

Figure 3-5 shows aRPD leveling off at 1.1 cm. Rounding this, we set our D-band at aRPD <1 cm.

Sutula et al. (2014) also defined a ‘cut value’ for TOC which separated reference sites from non-reference sites of 0.46% TOC (their Figure 3). Using the above equation, this equates to an aRPD of ~ 4.0 cm. We therefore took the A band for aRPD being > 4.0 cm. We set the B/C threshold at 2.5 cm, being mid-way between the A and D bands.

Sutula et al. (2014) showed considerable scatter in the TOC vs aRPD relationship. To calculate probability tables, a standard deviation of ± 2 cm is allowed for which spreads the probability distributions, selected by referring to the spread in values at non-reference sites from Sutula et al. (2014). A table relating TOC to aRPD was calculated as follows:

- For the four TOC bands (0.0-0.5%, 0.5 to 1.2%, 1.2 to 2%, 2 to 10% described in Table 3-11, 1000 TOC values (linearly spaced) were taken within each band;
- aRPD was estimated using $aRPD = 5.8 - 3.84 \text{ TOC} + \text{err}$, where err is a random number from a normal distribution with a standard deviation of 2 cm;
- The number of predicted aRPD values within each aRPD band (>4cm, 2.5-4cm, 1-2.5cm, <1cm) was counted, and the counts normalized to give the a % probability distribution for that TOC range.

This gave Table 3-12.

Table 3-12: Predicted effects of %TOC on aRPD.

Parent node state	State % probabilities: aRPD (cm)			
	>4	2.5 to 4	1 to 2.5	<1
%TOC				
0 to 0.5	65.3	21.5	9.9	3.3
0.5 to 1.2	24.7	25.9	25.6	23.8
1.2 to 2.0	2.3	7.5	17.4	72.8
2.0 to 10.0	0.0	0.1	0.8	99.1

In terms of macroalgal effects on aRPD, Sutula et al. (2014) showed a transition away from a ‘reference condition’ of negligible effect, occurring at ~15 g dw macroalgae/m². At the other end of the scale, severe adverse effects on aRPD were shown at an ‘exhaustion threshold’ (aRPD ~ 0) of ~175 g dw macroalgae/m² (the 5th percentile of the X intercept between macroalgal biomass and aRPD). Further work on California estuaries by Green et al. (2014) showed an intermediate point between these ‘reference’ and ‘exhaustion’ effects of macroalgae on macrofauna located ~110 g dw macroalgae/m². On this basis, we selected 15 g dw macroalgae/m² as the A/B threshold occurring at 4 cm aRPD, 110 g dw macroalgae/m² as the C/D threshold occurring at 1 cm aRPD, and 175 g dw macroalgae/m² occurring at 0 cm aRPD.

The macroalgal dw values at reference, intermediate and exhaustion thresholds were then converted to macroalgal EQR using a macroalgal dw to ww conversion factor (1/0.129: Sutula et al. (2014)) and ww to EQR using the band thresholds from Plew et al. (2020b) for ww of 0, 100, 200, 500, 1450 g macroalgae/m², equating to EQR scores of 1.0, 0.8, 0.6, 0.4 and 0.2, respectively. Relationships of these respective values are shown in Table 3-13.

Table 3-13: Relationships between aRPD, macroalgal dry weight, macroalgal wet weight and EQR.

aRPD (cm)	Dry weight (g/m ²)	Wet weight (g/m ²)	EQR
4	15	116	0.767
1	110	853	0.326
0	175	1357	0.220

Plotting EQR vs aRPD yielded a regression prediction of aRPD = 7.1535 EQR - 1.4637 ($r^2 = 0.996$). A probability distribution table (Table 3-14) linking EQR and aRPD was calculated in the same manner as that linking TOC and aRPD (again with a ±2 cm standard deviation included to spread out the probability distributions).

Table 3-14: Predicted effects of EQR on aRPD.

Parent node state EQR	State % probabilities: aRPD (cm)			
	>4	2.5 to 4	1 to 2.5	<1
0.8 to 1.0	69.0	20.0	8.5	2.5
0.6 to 0.8	41.8	28.4	19.6	10.2
0.4 to 0.6	18.1	25.1	28	28.8
<0.4	3.1	9.2	19.7	68

Finally, tables Table 3-12 and Table 3-14 were cross-multiplied to create the two-way CPT relating macroalgal EQR and %TOC to aRPD (Table 3-15).

Table 3-15: Predicted effects of EQR and %TOC on aRPD.

Parent node state		State % probabilities: aRPD (cm)			
EQR	%TOC	>4	2.5 to 4	1 to 2.5	<1
0.8 to 1.0	0 to 0.5%	89.6	8.5	1.7	0.2
0.8 to 1.0	0.5 to 1.2%	68.2	20.7	8.7	2.4
0.8 to 1.0	1.2 to 2.0%	24.8	23.5	23.2	28.5
0.8 to 1.0	2.0 to 10.0%	0	0.8	2.6	96.6
0.6 to 0.8	0 to 0.5%	76.5	17.1	5.4	1.0
0.6 to 0.8	0.5 to 1.2%	41.1	29.3	20.0	9.6
0.6 to 0.8	1.2 to 2.0%	6.9	15.3	24.5	53.3
0.6 to 0.8	2.0 to 10.0%	0	0.3	1.5	98.2
0.4 to 0.6	0 to 0.5%	56.5	25.8	13.2	4.5
0.4 to 0.6	0.5 to 1.2%	17.9	26.0	28.7	27.4
0.4 to 0.6	1.2 to 2.0%	1.5	6.7	17.3	74.5
0.4 to 0.6	2.0 to 10.0%	0	0.1	0.8	99.1
<0.4	0 to 0.5%	24.7	24.1	23.8	27.4
<0.4	0.5 to 1.2%	3.1	9.8	20.7	66.4
<0.4	1.2 to 2.0%	0.1	1.3	6.4	92.2
<0.4	2.0 to 10.0%	0	0.1	0.2	99.7

3.9 Macroalgae / mud / TOC / macrobenthos

As described for previous CPTs, eutrophication in shallow estuaries is often associated with excessive macroalgal biomass, high organic carbon in sediments, and excessive muddiness. These stressors can act synergistically to affect the health of macrobenthos in estuaries, by smothering animals and by creating anoxic and sulphidic conditions in their sedimentary environments (Green et al. 2014; Robertson et al. 2015; Robertson et al. 2016).

Robertson et al. (2016c) developed regression trees that identified threshold values of %mud and %TOC, at sampling sites where macroinvertebrate samples were taken, that delimited macrobenthic taxon abundance and richness for quantitatively determined macrobenthic ecological groups, sampled in 21 NZ SIDE and SSRTRE estuaries. The regression trees, which individually explained >95% of the total variance, delineated %mud at various levels (tree splits at ~12, ~25 and ~34 %mud, as primary in distinguishing abundance and diversity of the groups. In terms of benthic condition, AMBI Biotic Coefficients (BCs) ranged from 'Normal' (BC 1.2 – 3.3) to 'Transitional to pollution' (BC 3.3 – 4.3), to 'Polluted' (BC > 4.3). With increasing %mud, AMBI scores increased, indicating decreasing abundances and species richness of sensitive taxa (Ecological Groups I & II) and increasing abundances and richness of tolerant taxa (Ecological Groups IV & V). %TOC values were only important as a split criterion for abundance and richness indices if mud content was very high (>~34% for abundance and >~42% for richness), indicating organic enrichment rather than muddiness was the primary stressor for that split, and corresponded with %TOC values exceeding 1.2% within the 'Transitional to pollution' B-C band. Robertson et al. (2016c) concluded that the locally (NZ) calibrated AMBI provided a robust proxy of stress relating to the two dominant issues affecting macrobenthic communities in these systems, sediment mud content and organic enrichment.

Green et al. (2014) distinguished macroalgal eutrophication effects on macrobenthic health on intertidal flats in two California SIDE type lagoons. They described research indicating macroalgal biomasses below 15 g dw/m² had no negative effects on macrofauna, while a value of 110 g dw/m² was an approximate midpoint between ‘no effect’ and an ‘exhaustion threshold’ occurring at ~185 g dw/m². The latter value corresponded well with the value of 175 g dw/m² found by Sutula et al. (2014) for an exhaustion threshold for aRPD (section 3.8).

In combining the three variables (macroalgal EQR, %TOC and %mud) in the macrobenthic CPT, and accounting for the above considerations, we set %mud to have increasing impacts at levels of <12%, 12 to <25%, 25 to <34% and >34%, and considering the quartile ranges shown in Figure 7 of Robertson et al. (2016c) for abundance-weighted AMBI. We set %TOC to have increasing influence only after levels of %mud exceeded 34% and after levels of macroalgal EQR were < 0.4 (equivalent to ~65 g dw/m²). Macroalgal biomass had no influence at levels of EQR at ≥0.8 (equivalent to ~13 g dw/m²) and had increasing influence at EQR <0.8, where it corresponded to values exceeding reference conditions of Green et al. (2014).

Table 3-16: Predicted effects of macroalgal EQR, %TOC and %mud on AMBI Biotic Coefficients (BC's).

Parent node state			State % probabilities: AMBI BC's			
Macroalgal EQR	%TOC	%mud	<=1.2	>1.2-3.3	>3.3-4.3	>4.3-7
0.8 to 1	0 to 0.5	<12%	50	50	0	0
0.8 to 1	0 to 0.5	12-<25%	25	75	0	0
0.8 to 1	0 to 0.5	25-<34%	0	100	0	0
0.8 to 1	0 to 0.5	>34%	0	100	0	0
0.8 to 1	0.5 to 1.2	<12%	50	50	0	0
0.8 to 1	0.5 to 1.2	12-<25%	25	75	0	0
0.8 to 1	0.5 to 1.2	25-<34%	0	100	0	0
0.8 to 1	0.5 to 1.2	>34%	0	100	0	0
0.8 to 1	1.2 to 2	<12%	50	50	0	0
0.8 to 1	1.2 to 2	12-<25%	25	75	0	0
0.8 to 1	1.2 to 2	25-<34%	0	50	50	0
0.8 to 1	1.2 to 2	>34%	0	25	50	25
0.8 to 1	2 to 10	<12%	50	50	0	0
0.8 to 1	2 to 10	12-<25%	25	75	0	0
0.8 to 1	2 to 10	25-<34%	0	50	50	0
0.8 to 1	2 to 10	>34%	0	25	50	25
0.6 to <0.8	0 to 0.5	<12%	50	50	0	0
0.6 to <0.8	0 to 0.5	12-<25%	25	75	0	0
0.6 to <0.8	0 to 0.5	25-<34%	0	100	0	0
0.6 to <0.8	0 to 0.5	>34%	0	100	0	0
0.6 to <0.8	0.5 to 1.2	<12%	50	50	0	0
0.6 to <0.8	0.5 to 1.2	12-<25%	25	75	0	0
0.6 to <0.8	0.5 to 1.2	25-<34%	0	100	0	0
0.6 to <0.8	0.5 to 1.2	>34%	0	100	0	0
0.6 to <0.8	1.2 to 2	<12%	50	50	0	0
0.6 to <0.8	1.2 to 2	12-<25%	25	75	0	0
0.6 to <0.8	1.2 to 2	25-<34%	0	50	50	0
0.6 to <0.8	1.2 to 2	>34%	0	25	50	25

Parent node state			State % probabilities: AMBI BC's			
Macroalgal EQR	%TOC	%mud	<=1.2	>1.2-3.3	>3.3-4.3	>4.3-7
0.6 to <0.8	2 to 10	<12%	50	50	0	0
0.6 to <0.8	2 to 10	12-<25%	25	75	0	0
0.6 to <0.8	2 to 10	25-<34%	0	50	50	0
0.6 to <0.8	2 to 10	>34%	0	25	50	25
0.4 to <0.6	0 to 0.5	<12%	25	75	0	0
0.4 to <0.6	0 to 0.5	12-<25%	25	50	25	0
0.4 to <0.6	0 to 0.5	25-<34%	0	25	50	25
0.4 to <0.6	0 to 0.5	>34%	0	0	50	50
0.4 to <0.6	0.5 to 1.2	<12%	25	75	0	0
0.4 to <0.6	0.5 to 1.2	12-<25%	25	50	25	0
0.4 to <0.6	0.5 to 1.2	25-<34%	0	25	50	25
0.4 to <0.6	0.5 to 1.2	>34%	0	0	50	50
0.4 to <0.6	1.2 to 2	<12%	25	75	0	0
0.4 to <0.6	1.2 to 2	12-<25%	25	50	25	0
0.4 to <0.6	1.2 to 2	25-<34%	0	25	50	25
0.4 to <0.6	1.2 to 2	>34%	0	0	50	50
0.4 to <0.6	2 to 10	<12%	25	75	0	0
0.4 to <0.6	2 to 10	12-<25%	25	50	25	0
0.4 to <0.6	2 to 10	25-<34%	0	25	50	25
0.4 to <0.6	2 to 10	>34%	0	0	50	50
0 to <0.4	0 to 0.5	<12%	0	25	75	0
0 to <0.4	0 to 0.5	12-<25%	0	25	50	25
0 to <0.4	0 to 0.5	25-<34%	0	0	75	25
0 to <0.4	0 to 0.5	>34%	0	0	50	50
0 to <0.4	0.5 to 1.2	<12%	0	25	75	0
0 to <0.4	0.5 to 1.2	12-<25%	0	25	50	25
0 to <0.4	0.5 to 1.2	25-<34%	0	0	75	25
0 to <0.4	0.5 to 1.2	>34%	0	0	50	50
0 to <0.4	1.2 to 2	<12%	0	25	50	25
0 to <0.4	1.2 to 2	12-<25%	0	0	50	50
0 to <0.4	1.2 to 2	25-<34%	0	0	25	75
0 to <0.4	1.2 to 2	>34%	0	0	0	100
0 to <0.4	2 to 10	<12%	0	25	50	25
0 to <0.4	2 to 10	12-<25%	0	0	50	50
0 to <0.4	2 to 10	25-<34%	0	0	25	75
0 to <0.4	2 to 10	>34%	0	0	0	100

3.10 Stratification / estuary type / flushing / phytoplankton / oxygen

Oxygen-requiring (aerobic) estuarine organisms use environmental oxygen (O₂) to extract energy from organic matter, to survive and grow (Lehninger 1975). As organic matter is consumed it is respired, turning O₂ into water and thus reducing its levels in the environment. When O₂ reduction becomes greater than its replenishment by photosynthesis or hydrodynamic and atmospheric exchange, its concentrations are reduced and can become stressful for biota (Gray et al. 2002;

Vaquer-Sunyer and Duarte 2008; Vaquer-Sunyer and Duarte 2011). In extreme cases, this de-oxygenation (hypoxia) can be catastrophic for biota and normal biogeochemical functioning of coastal ecosystems (Conley et al. 2009; NRC 2000; Sutula 2011). Because of its importance for estuary health, Sutula (2011) considered the O₂ indicator to have highly beneficial uses in estuary management, with well-validated means of measurement and acceptable measurement precision for eutrophication assessment.

Susceptibility to hypoxia in estuaries is conditioned by both biological and physical effects (Scully 2016). Biological effects have been demonstrated by O₂ responses to phytoplankton seasonality (Harding et al. 2014), as the net primary production of spring and summer is consumed later in the summer and autumn by net microbial respiration (Wallace et al. 2014; Zeldis and Swaney 2018). This dependence on primary production indicates that the extent of O₂ depletion can be a positive function of nutrient inputs and phytoplankton biomass during the production season (Harding et al. 2014; Hughes et al. 2011; NRC 2000; Wallace et al. 2014). For regulatory purposes, achievement of desired levels of O₂ has therefore been tied to limits of phytoplankton biomass (often measured as chl-*a*; e.g., Harding et al. (2014)).

Physical processes affect hypoxic susceptibility via estuary stratification and residence time effects. Low O₂ can occur in deeper estuaries if the water column becomes density-stratified, acting to isolate the deeper layers from atmospheric exchange (NRC 2000; Scully 2016). On the other hand, if the water column is shallow or regularly vertically mixed, atmospheric exchange is maintained and hypoxic conditions will generally not form. The formation of low O₂ conditions in estuaries is also governed by turnover time, with longer flushing times more likely to sustain low O₂ waters. These physiographic effects mean that O₂ conditions in estuaries can depend strongly on estuary type. Shallow, well mixed systems such as tidal lagoons (SIDEs) or river estuaries (SSRTREs) are less likely to exhibit low O₂, unless they include deep holes which support stratification. Deep, large bay systems (DSDEs) are more likely to be susceptible to O₂ depletion because they regularly stratify, especially later in the production season, and because they have relatively long flushing times.

Given these interacting controls on estuary O₂ levels, the CPT governing estuary O₂ levels in the BBN was conditioned by states of physical and biological parent nodes that evaluated stratification likelihood, estuary type, phytoplankton biomass and flushing times. To simplify the Oxygen CPT, stratification and estuary type inputs were combined in an intermediate 'Oxygen depletion susceptibility' calculation node (Figure 2-1) that prescribed whether the various estuary types are susceptible to high, medium or low O₂ depletion, depending on whether they are stratified. This susceptibility, along with chl-*a* levels and flushing time, were then input to the Oxygen node (Figure 2-1) to predict O₂ levels in the estuaries.

The O₂ bandings applied in the Oxygen CPT (Table 3-17) were set using the 7 day mean minimum thresholds given in Robertson et al. (2016b) (their Table 7), which were based on NZ National Objective Framework (NOF) criteria for rivers (Davies-Colley et al. 2013) and California estuary criteria (Sutula et al. 2012). This identified dissolved O₂ levels ranging from no stress/minor stress on aquatic organisms at O₂ levels ≥ 7 mg/L, to significant, persistent stress with likelihood of local extinctions and loss of ecological integrity at <5.0 mg/L.

Table 3-17: Ecological conditions associated with the bandings (A – D) of the Oxygen node of the BBN.
Adapted from Robertson et al. (2016b).

Band	A	B	C	D
Ecological quality	No stress caused by low O ₂ on any aquatic organisms that are present at near-pristine sites	Occasional minor stress on sensitive organisms caused by short periods (a few hours each day) of lower O ₂ . Risk of reduced abundance, performance and welfare of sensitive fish and macroinvertebrate species.	Moderate stress on a number of aquatic organisms caused by O ₂ levels less than preference levels for periods of several hours each day. Risk of sensitive fish and macroinvertebrate species being lost.	Significant, persistent stress on a range of aquatic organisms caused by O ₂ less than tolerance levels. Likelihood of local extinctions of keystone species and loss of ecological integrity.
7 day mean minimum	≥7.0 mg/l	7.0 - ≥6.0 mg/l	6.0 - ≥5.0 mg/l	<5.0 mg/l

Further consideration can be made of the band settings of Table 3-17. The review of Vaquer-Sunyer and Duarte (2008) questioned the widespread use of the 2 mg O₂/L threshold in conventional applications and recommended its upward revision. They showed that this historically commonly used threshold is below the empirical sublethal and lethal O₂ thresholds for half the macrofaunal species they examined. A level of 4.6 mg O₂/L was recommended as ‘a precautionary limit to avoid catastrophic mortality events, except for the most sensitive (e.g., crab) species, and to effectively preserve biodiversity’. Sheldon and Alber (2010) designated dissolved O₂ criteria for Georgia (USA) estuary waters based on the NEEA assessment for US estuaries of Bricker et al. (2003). They designated 3.0 mg O₂/L for a ‘fair/poor’ threshold and 5.5 mg O₂/L for a ‘good/fair’ threshold.

Batiuk et al. (2009) designated dissolved O₂ criteria for Chesapeake Bay (USA) for protection of individual ecological values (e.g., fisheries, habitat protection including larval recruitment, bivalve fisheries) in its individual sub-regions. The Chesapeake Bay O₂ criteria were developed by accounting for the temporal and spatial complexity of both the biotic communities of the Bay and the susceptibility to O₂ depletion of its various habitats. Criteria to protect against adverse effects included a 30-day mean of 5 mg O₂/L applied to open-water habitats, and a 7-day mean of 4 mg O₂/L. Sutula et al. (2012) recommended a value of 5.8 mg/L as a minimum threshold for chronic exposure, protective of lethal and sublethal effects, long-term for California estuaries (exclusive of salmonids).

Zeldis et al. (2015) reviewed O₂ limits for health of key NZ aquaculture species (Greenshell mussels, salmon, Kingfish). In summary, this review indicated that O₂ levels less than 6 mg/L are undesirable and those less than 5.3 mg/L should be interpreted as precautionary levels to be avoided. The higher level was in approximate agreement with the salmonid limits suggested by Sutula et al. (2012).

In addition to faunal responses to hypoxia, the biogeochemical environment itself also displays identifiable thresholds of response to O₂ levels. Coupled denitrification in estuarine sediments involves a finely balanced relationship between aerobic and anaerobic bacterial communities in proximity in surficial sediments (Sutula 2011) and it can be limited by conditions of organic

enrichment of sediments and low bottom water O₂. Resulting low redox conditions and shallow penetration of O₂ into sediments inhibit nitrification, and consequently denitrification, allowing more of the organic N deposited to sediments to be returned to the water column as ammonium rather than vented to the atmosphere as N₂ gas (Kemp et al. 1990). Boynton and Kemp (2008) concluded that at bottom water O₂ of <5 mg O₂/L, 80% of effluxed N was ammonium (rather than N₂) while at >6 mg O₂/L this dropped to 60%.

Oxygen management criteria adopted by NZ regional councils include Horizons Regional Council's 'One Plan', stating that minimum O₂ saturation standards for its estuary management subzone should be 70% saturation³ (5.3 mg/L)⁴. A level of 80% saturation (6.1 mg/L) has been recommended in Waikato Regional Council standards to avoid unsatisfactory conditions for plants and animals⁵, although it is not clear that this is to be applied to marine waters.

Overall, these considerations of overseas and local criteria suggest that the band settings used the BBN (Table 3-17) are appropriate for identifying estuarine O₂ concentrations ranging from those that will support ecological conditions ranging from healthy to very compromised, in NZ estuaries.

The methods used to link the Stratification, Estuary type, Flushing and Phytoplankton nodes to the Oxygen node (Table 3-18, Table 3-19) were as follows. For DSDEs, field data from the Firth of Thames long-term mooring site (Zeldis and Swaney 2018) on apparent oxygen utilisation (AOU)⁶ were obtained from the upper mixed layer of the water column (10 m depth) and below, in seasonally-stratified waters (33 m depth) (Figure 3-6). Data were collected between July 2011 and October 2017 for temperature, salinity and O₂ concentration using Seabird MicroCAT (SBE-37-ODO) instruments measuring at 15 min. intervals⁷. To derive a relationship between AOU and phytoplankton biomass in its deeper stratified waters, AOU data were compared with chl-*a* data collected near the mooring in the lower water column (≥20 m). Median AOU values from the summer season (December through February) when AOU is maximal (Figure 3-6; Zeldis and Swaney (2018)) were compared with median chl-*a* values obtained from spring through summer (September through February). This was on the assumption that it is accumulated spring and summer phytoplankton biomass that influences summer O₂ drawdown. The resulting chl-*a* specific O₂ utilisation rate (mg O₂/mg chl-*a*) was converted to a daily rate by dividing by the Firth water residence time, estimated using a mixing model estimate of summer residence time of 35 d (Zeldis and Swaney 2018). This gave a summer O₂ utilization rate of 42 mg O₂/mg chl-*a*/d⁻¹ in the deeper, stratified water. This was considered the chl-*a* -specific rate of drawdown to be expected under stratified conditions in summer, in DSDEs (such as the Firth).

To derive chl-*a* -specific O₂ drawdown rates in stratified conditions for SIDES, SSRTREs and coastal lakes, data from detailed vertical profiles of water column properties (O₂, chl-*a*, temperature, salinity) of Ohau Estuary (Manawatu) were used (L. Stevens, Salt Ecology, November 2020, pers.

³ <http://www.horizons.govt.nz/assets/publications/about-us-publications/one-plan-publications-and-reports/proposed-one-plan/ScheduleH.pdf>

⁴ Converted using <https://www.loligosystems.com/convert-oxygen-units> assuming typical conditions of 20°C, 30 psu and 1013 hPa.

⁵ <https://www.waikatoregion.govt.nz/Environment/Natural-resources/Water/Rivers/healthyrivers/Water-quality-glossary/>

⁶ In freshwater or marine systems apparent oxygen utilisation (AOU) is the difference between the measured dissolved O₂ concentration and its equilibrium saturated concentration in water with the same physical and chemical properties. It measures how processes such as respiration and primary production alter O₂ concentrations *in situ*.

⁷ The instruments were factory-calibrated at the calibration interval (2 years) recommended by the manufacturer. Drift in O₂ records during deployment periods arising from biofouling was corrected assuming linear drift from reference values (taken after deployment of cleaned instruments). Further details of calibrations and validations for these O₂ data are given in Zeldis et al. (2015).

comm.). Flushing time for this estuary (0.61 d) was obtained from ETI Tool 1. The resulting value used from this dataset was 1 mg O₂/mg chl-*a*/d, which was used in the BBN to constrain chl-*a* -specific O₂ depletion expected in stratified waters of SIDES, SSRTREs and coastal lakes.

To derive O₂ depletion in non-stratified systems (for all estuary types), the median AOU value in the upper water column of the Firth was used, with flushing time set at 0.5 day. This was on the assumption that drawdown will cause net O₂ depletion only at night, when there is no photosynthesis. The chl-*a* specific rate (calculated as above using the 7 m depth microcat and chl-*a* data from <20 m depth) was 6 mg O₂/mg chl-*a*. This is a daily rate, so it was doubled to 12 mg O₂/mg chl-*a*, to obtain the drawdown occurring only at night.

For the two stratified cases, O₂ consumption is calculated as the greater of either:

$$\text{AOU} * \text{chl-}a * \text{flushing time or}$$

$$\text{AOUs} * \text{chl-}a * 0.5,$$

where AOU is the high or medium AOU rate (mg O₂/mg chl-*a*/d), and AOUs is the rate for non-stratified systems (12 mg O₂/mg chl-*a*/d). This calculation step modifies the Oxygen CPT for the medium susceptibility case and is a correction that prevents a non-stratified system having greater O₂ depletion than a stratified system for short flushing times.

The lower chl-*a* specific AOU described above for SIDES, SSRTREs and coastal lakes than for DSDEs is likely due to their shallowness, generally short flushing times and higher light levels at depth, giving more primary production (O₂ production). DSDEs appear to be very susceptible to O₂ depletion, as evidenced by the chl-*a* -specific AOU for the Firth shown here. This is similar to responses seen in Chesapeake Bay (USA), where severe hypoxia is accompanied by mean chl-*a* levels in its mesohaline reaches about 8 mg chl-*a*/m³ (Kemp et al. 2005). Mean chl-*a* criteria for the mesohaline reaches of Chesapeake Bay ranging from 2.2 to 8.7 mg chl-*a*/m³ (depending on season and river flow) have been recommended (Harding et al. 2014) for achieving restoration targets, while 90th percentile threshold values that should rarely be exceeded ranged from 6.9-27 mg chl-*a*/m³. Values somewhat lower than these were recommended for the polyhaline (seaward) reaches. These values are not much greater than 90th percentile values observed at inner Firth sites (J. Zeldis unpubl. data). It is likely that the physiography of Chesapeake Bay (relatively clear waters, long residence times, heavy nutrient loading) renders it susceptible to blooms, and its similarity in that regard with the Firth suggests why the Firth is susceptible as well.

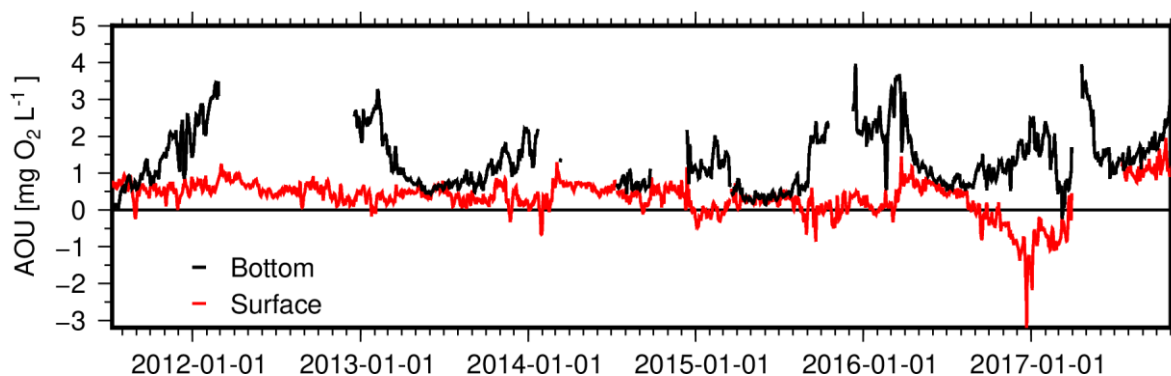


Figure 3-6: Apparent oxygen utilisation (AOU: mg/L) results from the biophysical mooring at the outer (40 m depth) Firth of Thames location, from 2011 to 2017. The mooring carried Seabird microcat temperature/salinity/O₂ instruments at near-surface (red trace) and near-bottom (black trace) water column depths. Gaps in the records were due to instrument failures.

Table 3-18: Predicted effects of stratification and estuary type on O₂ depletion susceptibility.

Parent node state		State: O ₂ depletion susceptibility
Stratified	Estuary Type	
Yes	DSDE	High
Yes	SIDE	Medium
Yes	SSRTRE	Medium
Yes	Coastal Lake	Medium
No	DSDE	Low
No	SIDE	Low
No	SSRTRE	Low
No	Coastal Lake	Low

Table 3-19: Predicted effects of O₂ depletion susceptibility, chl-*a* biomass (mg/L) and estuary flushing time (d) on estuary O₂ levels (mg/L). Oxygen concentrations were calculated using chl-*a* -specific drawdown rates described in text, assuming a starting saturated O₂ concentration of 7.5 mg/L.

Parent node state			State % probabilities: O ₂			
O ₂ depletion susceptibility	Chl- <i>a</i>	Flushing Time	≥7.0 mg/l	≥6.0 mg/l	≥5.0 mg/l	<5.0 mg/l
High	0 to 5	0 to 3	95.2	4.8	0	0
High	0 to 5	3 to 6	51.3	48.7	0	0
High	0 to 5	6 to 10	31.7	50.2	18.1	0
High	0 to 5	>10	12.6	16.8	16.5	54.1
High	5 to 10	0 to 3	52	48	0	0
High	5 to 10	3 to 6	0	53.5	44.6	1.9
High	5 to 10	6 to 10	0	1.8	41.2	57
High	5 to 10	>10	0	0	0.4	99.6
High	10 to 15	0 to 3	30.4	58.3	11.3	0
High	10 to 15	3 to 6	0	1.9	48.9	49.2
High	10 to 15	6 to 10	0	0	0	100
High	10 to 15	>10	0	0	0	100
High	15 to 25	0 to 3	19.3	37.8	33.1	9.8
High	15 to 25	3 to 6	0	0	4.9	95.1

Parent node state			State % probabilities: O ₂			
O ₂ depletion susceptibility	Chl- <i>a</i>	Flushing Time	≥7.0 mg/l	≥6.0 mg/l	≥5.0 mg/l	<5.0 mg/l
High	15 to 25	6 to 10	0	0	0	100
High	15 to 25	>10	0	0	0	100
High	25 to 60	0 to 3	10	18.6	18.5	52.9
High	25 to 60	3 to 6	0	0	0	100
High	25 to 60	6 to 10	0	0	0	100
High	25 to 60	>10	0	0	0	100
High	60 to 100	0 to 3	4.9	8.5	8.6	78
High	60 to 100	3 to 6	0	0	0	100
High	60 to 100	6 to 10	0	0	0	100
High	60 to 100	>10	0	0	0	100
Medium	0 to 5	0 to 3	100	0	0	0
Medium	0 to 5	3 to 6	100	0	0	0
Medium	0 to 5	6 to 10	100	0	0	0
Medium	0 to 5	>10	100	0	0	0
Medium	5 to 10	0 to 3	100	0	0	0
Medium	5 to 10	3 to 6	100	0	0	0
Medium	5 to 10	6 to 10	100	0	0	0
Medium	5 to 10	>10	62.3	37.7	0	0
Medium	10 to 15	0 to 3	100	0	0	0
Medium	10 to 15	3 to 6	100	0	0	0
Medium	10 to 15	6 to 10	100	0	0	0
Medium	10 to 15	>10	26	74	0	0
Medium	15 to 25	0 to 3	100	0	0	0
Medium	15 to 25	3 to 6	100	0	0	0
Medium	15 to 25	6 to 10	100	0	0	0
Medium	15 to 25	>10	7.7	63.3	29	0
Medium	25 to 60	0 to 3	100	0	0	0
Medium	25 to 60	3 to 6	80.6	19.4	0	0
Medium	25 to 60	6 to 10	23.3	76.7	0	0
Medium	25 to 60	>10	0.1	22.8	31.4	45.7
Medium	60 to 100	0 to 3	88.8	11.2	0	0
Medium	60 to 100	3 to 6	8.3	91.7	0	0
Medium	60 to 100	6 to 10	0	58.8	41.2	0
Medium	60 to 100	>10	0	1.2	10.6	88.2
Low	0 to 5	0 to 3	100	0	0	0
Low	0 to 5	3 to 6	100	0	0	0
Low	0 to 5	6 to 10	100	0	0	0
Low	0 to 5	>10	100	0	0	0
Low	5 to 10	0 to 3	100	0	0	0
Low	5 to 10	3 to 6	100	0	0	0
Low	5 to 10	6 to 10	100	0	0	0
Low	5 to 10	>10	100	0	0	0
Low	10 to 15	0 to 3	100	0	0	0
Low	10 to 15	3 to 6	100	0	0	0

Parent node state			State % probabilities: O ₂			
O ₂ depletion susceptibility	Chl- <i>a</i>	Flushing Time	≥7.0 mg/l	≥6.0 mg/l	≥5.0 mg/l	<5.0 mg/l
Low	10 to 15	6 to 10	100	0	0	0
Low	10 to 15	>10	100	0	0	0
Low	15 to 25	0 to 3	100	0	0	0
Low	15 to 25	3 to 6	100	0	0	0
Low	15 to 25	6 to 10	100	0	0	0
Low	15 to 25	>10	100	0	0	0
Low	25 to 60	0 to 3	100	0	0	0
Low	25 to 60	3 to 6	100	0	0	0
Low	25 to 60	6 to 10	100	0	0	0
Low	25 to 60	>10	100	0	0	0
Low	60 to 100	0 to 3	40	60	0	0
Low	60 to 100	3 to 6	40	60	0	0
Low	60 to 100	6 to 10	40	60	0	0
Low	60 to 100	>10	40	60	0	0

3.11 Potential N concentration / mud / seagrass

Seagrasses (*Zostera muelleri*) are vascular, rooted estuarine macrophytes that are keystone ecological components of historically healthy NZ estuaries (Robertson et al. 2016a). They provide high value habitat for a wide range of biota (Morrison et al. 2009) and are also well-known as providers of key ecosystem services including wave attenuation, increased water clarity, denitrification and carbon sequestration (Duarte and Krause-Jensen 2018; Reynolds et al. 2016).

The presence of seagrass beds in good condition is generally considered to indicate low/moderate nutrient and mud inputs and good water quality, while large scale seagrass losses have been documented where these conditions have not been met (Inglis 2003; Morrison et al. 2009; Park 1999). In some shallow NZ tidal lagoons, seagrass loss has been associated with smothering by excessive macroalgal cover (often in association with increased organic enrichment of sediments, low water clarity, poor oxygenation and increased muddiness) (Robertson et al. 2017; Stevens 2018a). In Southland estuaries, by far the most extensive seagrass losses have come in areas directly affected by excessive macroalgal growth and the deposition of mud-dominated sediments. For example, Stevens (2018a) reported a 94% reduction in dense seagrass in the Waihopai Arm in New River Estuary from 2001-2018, attributed primarily to smothering by fine sediments and nuisance macroalgal growths that initially established in 2007. Within Jacobs River Estuary there was a >80% loss from the highly eutrophic Pourakino Arm between 2003 and 2016, and Fortrose/Toetoes estuaries showed similar percentage losses because of smothering by macroalgae and fine sediment in the northern embayment by Titiroa Stream (Robertson et al. 2017; Stevens and Robertson 2017).

Orth et al. (2019) documented substantial improvements in seagrass health in US Atlantic coastal bays upon improvements in point source nutrient loadings, while Cloern (2001) summarized research showing large seagrass habitat loss in European systems with eutrophication. Similarly, Burkholder et al. (2007) showed that watershed N-loading to Sarasota Bay (Florida) had strong effects on seagrass biomass and productivity, with steep declines at elevated loading levels. These studies indicate a generalized eutrophication response that is consistent with the precipitous declines of seagrass in several NZ estuaries in recent years (e.g., New River, Jacobs River estuaries: Zeldis et al. (2019)) as N

loading levels have increased. In the Avon-Heathcote Estuary (Christchurch), seagrass bed recovery has been observed following diversion of the wastewater from the estuary (Gibson and Marsden 2016) commensurate with reductions in ammonium concentrations from ~ 20 to $3 \mu\text{mol}$ and substantial reductions in macroalgal cover and biomass (Barr et al. 2020). At high to very high N levels, toxicity effects appear to be important. Burkholder et al. (1994) showed that at nitrate concentrations of $80\text{-}170 \text{ mg/m}^3$ ($\sim 6\text{-}12 \mu\text{mol}$ nitrate) there were fatal toxicity effects on seagrass survival, and Katwijk et al. (1997) documented toxic effects at $\sim 25 \mu\text{mol}$ ammonium. The latter authors found no toxicity arising from nitrate effects, which they attributed to ammonium inhibition of nitrate uptake.

A threshold of 23% mud content, above which NZ seagrass does not occur, has been suggested by recent work in Porirua Harbour (Zabarte-Maeztu et al. 2019) although a lower threshold (13%) was indicated for Tauranga Harbour by Park and Donald (1994). Work in the USA (Chesapeake Bay) has observed the preferred sediment mud content for the larger species, *Zostera marina*, is 0.4%–30% mud content (Batuik et al. 2000), although Kemp et al. (2004) widened this range to 70%. It is also noted that historic seagrass beds in the Waihopai Arm of New River Estuary (Southland) were growing in sediments with mud contents *ca* 50-90% (Zeldis et al. 2019), (L. Stevens, Salt Ecology pers. obs.). Despite the high mud content these seagrass beds did not become displaced until they were overgrown with macroalgae (initially *Ulva* and then *Gracilaria*). Stevens (2018b) reported a similar situation in Westhaven Inlet (Tasman) with very extensive seagrass beds growing in sediments with >25% mud content for long periods (1990-2013) before undergoing a catastrophic reduction from 2013-2016. The cause for that decline is unclear but appears unrelated to catchment land use changes or macroalgal impacts.

Considering this information showing that seagrass habitat is affected by a variety of both eutrophication and non-eutrophication related stressors, it may be unrealistic to expect a consistent response of seagrass condition that matches nutrient and/or sediment loads in the various NZ estuary types (Robertson et al. 2016b). Irrespective, in constructing the seagrass CPT it was assumed that that nutrient loading (eutrophication) is a primary driver of seagrass condition. We assumed that potential TN levels $\geq 150\text{-}200 \text{ mg/m}^3$ ($\sim 10\text{-}14 \mu\text{mol}$) were likely to elicit macroalgal growths at the \geq B to C EQR band threshold (section 3.1), that would correspond to poor conditions for seagrass arising from both eutrophication and potential nitrate toxicity. We also assumed that N levels $\geq 300\text{-}450 \text{ mg/m}^3$ ($\sim 20\text{-}32 \mu\text{mol}$) would elicit severe toxicity effects if the TN was dominated by ammonium. Further, we assumed that %mud levels $\geq 25\text{-}34\%$ would elicit deleterious effects. The metric employed for assessing seagrass health was extent of seagrass cover as percentage of estimated natural state cover (ENSC: Robertson et al. 2016b), with values from 95% to 85% ENSC signifying moderate stress (C band) and <85% significant, persistent stress (D band).

Table 3-20: Predicted effects of Potential Total Nitrogen concentration (mg/m³) and %mud on seagrass. Metric is % of estuary with >20% seagrass cover compared to Estimated Natural State Cover (Robertson et al. 2016b).

Parent node state		State % probabilities: Seagrass % natural state			
Potential TN	%mud	<85	85-95	95-99	100
0 to 50	0 to 12	0	0	0	100
0 to 50	12 to 25	0	50	25	25
0 to 50	25 to 34	25	50	25	0
0 to 50	34 to 100	50	25	25	0
50 to 100	0 to 12	0	0	25	75
50 to 100	12 to 25	20	50	25	0
50 to 100	25 to 34	60	40	0	0
50 to 100	34 to 100	80	20	0	0
100 to 150	0 to 12	60	25	15	0
100 to 150	12 to 25	70	20	10	0
100 to 150	25 to 34	90	10	0	0
100 to 150	34 to 100	100	0	0	0
150 to 200	0 to 12	100	0	0	0
150 to 200	12 to 25	100	0	0	0
150 to 200	25 to 34	100	0	0	0
150 to 200	34 to 100	100	0	0	0
200 to 300	0 to 12	100	0	0	0
200 to 300	12 to 25	100	0	0	0
200 to 300	25 to 34	100	0	0	0
200 to 300	34 to 100	100	0	0	0
300 to 450	0 to 12	100	0	0	0
300 to 450	12 to 25	100	0	0	0
300 to 450	25 to 34	100	0	0	0
300 to 450	34 to 100	100	0	0	0
450 to 5000	0 to 12	100	0	0	0
450 to 5000	12 to 25	100	0	0	0
450 to 5000	25 to 34	100	0	0	0
450 to 5000	34 to 100	100	0	0	0

3.12 Indicator nodes / standardised nodes

These are included in the BBN to convert values resulting from each primary and secondary indicator node to a value between 0 and 16, prior to input to the primary and secondary score nodes (Figure 2-1). This is done because the thresholds between bands for the indicators are not evenly spread. This standardization step linearizes and normalizes each indicator score enabling the results of BBN to be directly compared with results of ETI Tool 2 for individual estuaries. This range was used in the ETI Tool 2 formulation, to enable a reasonably finely resolved spread across the range of scores obtained for each indicator (Zeldis et al. 2017c). Such standardization nodes are used throughout the BBN to map primary and secondary indicator values to their respective primary and secondary scoring nodes. They are visible in the example BBN models presented in section 4.

As an example of such a standardization, Table 3-21 shows the predicted macroalgal EQR (ranging between 0 and 1) mapped to the range of ETI primary scores (0-16). The previously shown Table 3-3 is another example, which in that case incorporates the modifying effect of salinity on how phytoplankton biomass is mapped to the primary scores.

Table 3-21: Example mapping of predicted macroalgal EQR to the range of ETI Primary scores (0-16).

Parent node states EQR	State: std. Macroalgae ETI Primary scores
0.8 to 1	0 to 4
0.6 to <0.8	4 to 8
0.4 to <0.6	8 to 12
0 to <0.4	12 to 16

3.13 Standardised primary nodes / ETI primary score

The ETI primary score CPT is calculated internally by Netica using an equation that selects the maximum of the standardised primary indicator values (either for macroalgae or phytoplankton):

$$ETI_pri (Macro_std, Phyto_std, intertidal) = \text{if}(\text{intertidal} < 5, \text{Phyto_std}, \text{if}(\text{intertidal} > 40, \text{Macro_std}, \text{if}(\text{Macro_std} > \text{Phyto_std}, \text{Macro_std}, \text{Phyto_std})))$$

This equation includes percent intertidal area to determine which of the two primary indicators to use in the primary indicator scoring. As described in section 3.3, if intertidal area is < 5%, phytoplankton is selected, if >40% macroalgae is selected and if between 5 and 40% the larger of the two is selected.

The ETI primary score node table which incorporates these settings and maps them to the various combinations of standardised macroalgae and phytoplankton scores is very large and is not shown here. However, it may be examined by opening that node in Netica using the ETI Tool 3 application and opening the 'Table' tab. This is also true for the ETI secondary score table, below.

3.14 Standardised secondary nodes / ETI secondary score

The ETI secondary score CPT is calculated internally by Netica using an equation that selects the average of standardised secondary indicator node scores using the equation:

$$ETI_sec (aRPD_std, Macrob_std, TOC_std, Seagrass_std, Oxygen_std) = \text{avg}(aRPD_std, Macrob_std, TOC_std, Seagrass_std, Oxygen_std)$$

3.15 ETI primary score and ETI secondary score / ETI final score

The ETI final score CPT is calculated internally by Netica using an equation that selects the average of the primary and secondary scores and normalizes it to between zero and one, using the equation:

$$ETI (ETI_sec, ETI_pri) = (ETI_pri + ETI_sec) / 32$$

4 Example BBN results

Here we present some example output from the ETI Tool 3 BBN. We first demonstrate the findings for a highly impacted estuary: Jacobs River Estuary (Southland), a SIDE – type estuary that is always open to the sea (Figure 4-1). In its current state of potential TN concentration and sediment loading, the probability distribution of results for ETI score shows this estuary is primarily in the D band of condition (highly impacted: Table 2-1). It has a very high potential TN concentration, and moderate sediment deposition rate. Its macroalgal EQR value is very low (very high eutrophication), it has very shallow aRPD in sediments, is muddy with high %TOC, poor seagrass condition and poor macrobenthos condition. Its water column O₂ levels are high however, because it is shallow and not stratified. This array of results is consistent with the poor ecological condition of Jacobs River Estuary documented in Zeldis et al. (2019) based on ecological surveys.

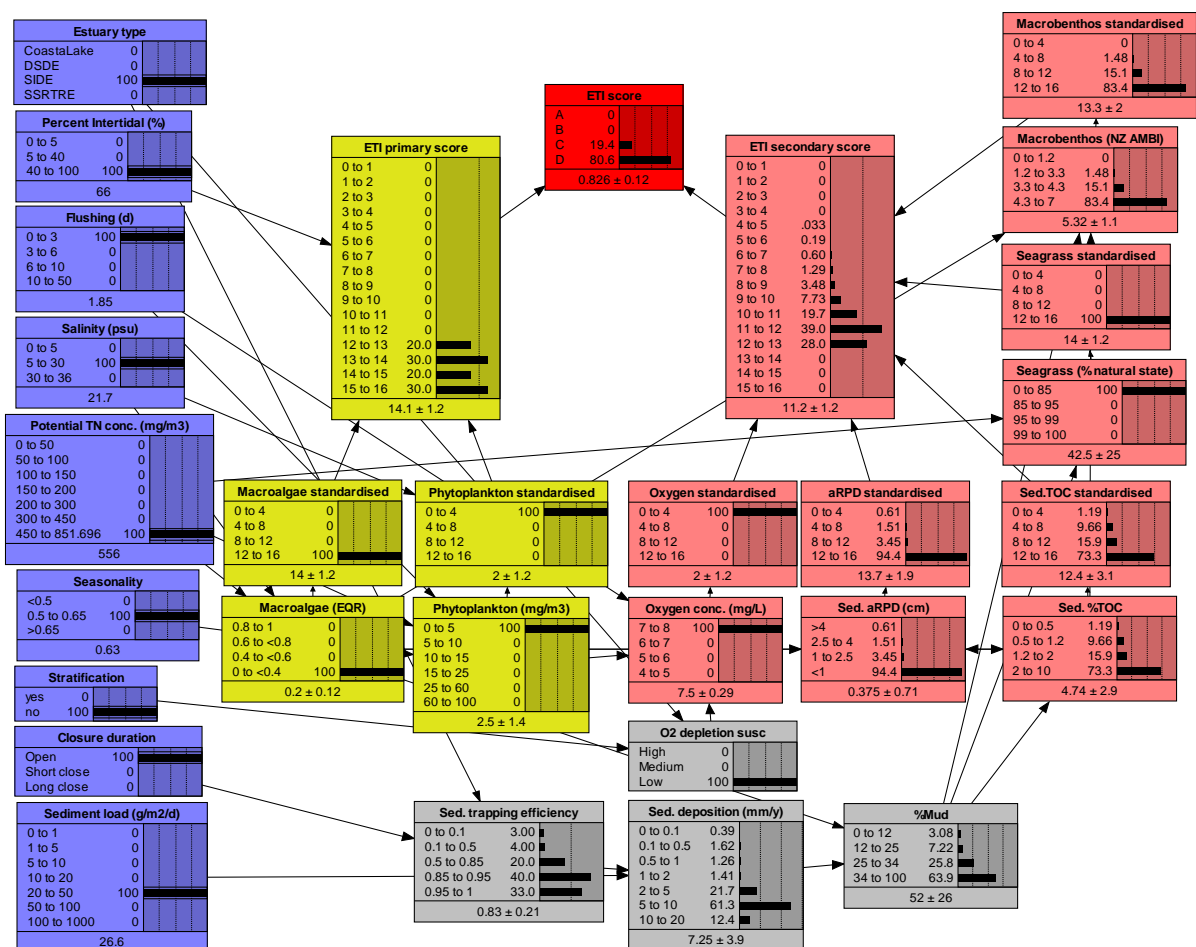


Figure 4-1: Netica BBN output for Jacobs River Estuary in its current state. Blue boxes are driver nodes with values input from ETI Tool 1, yellow and pink nodes are primary and secondary indicator nodes and the red node is the final ETI score. Grey nodes are intermediate calculation nodes. Indicator nodes that contribute to the scoring nodes have accompanying standardizing nodes (see text). This and following BBN runs employed “Netica v19.neta”.

We next show a BBN model run for Jacobs River Estuary with potential TN concentrations reduced by 66%, as a demonstration of predictive capability of the model (Figure 4-2). Many indicator node values are improved, including higher macroalgal EQR, deepened aRPD, reduced %TOC and improved AMBI and seagrass state. Its final ETI score distribution is centred on a ‘B’ condition (slight

eutrophication: Table 2-1). It is straightforward to translate these changes in potential TN to TN load reductions, using methods of Plew et al. (2018) and shown in Snelder et al. (2020). This demonstrates the utility of the BBN for informing upstream limit setting with respect to estuarine receiving environments. It is an example of how that by using BBN's, one can calculate not only the values of consequences (i.e., ETI scores or values of indicators) arising from causes (i.e., drivers), but also the values of different causes given the consequences (Uusitalo 2007).

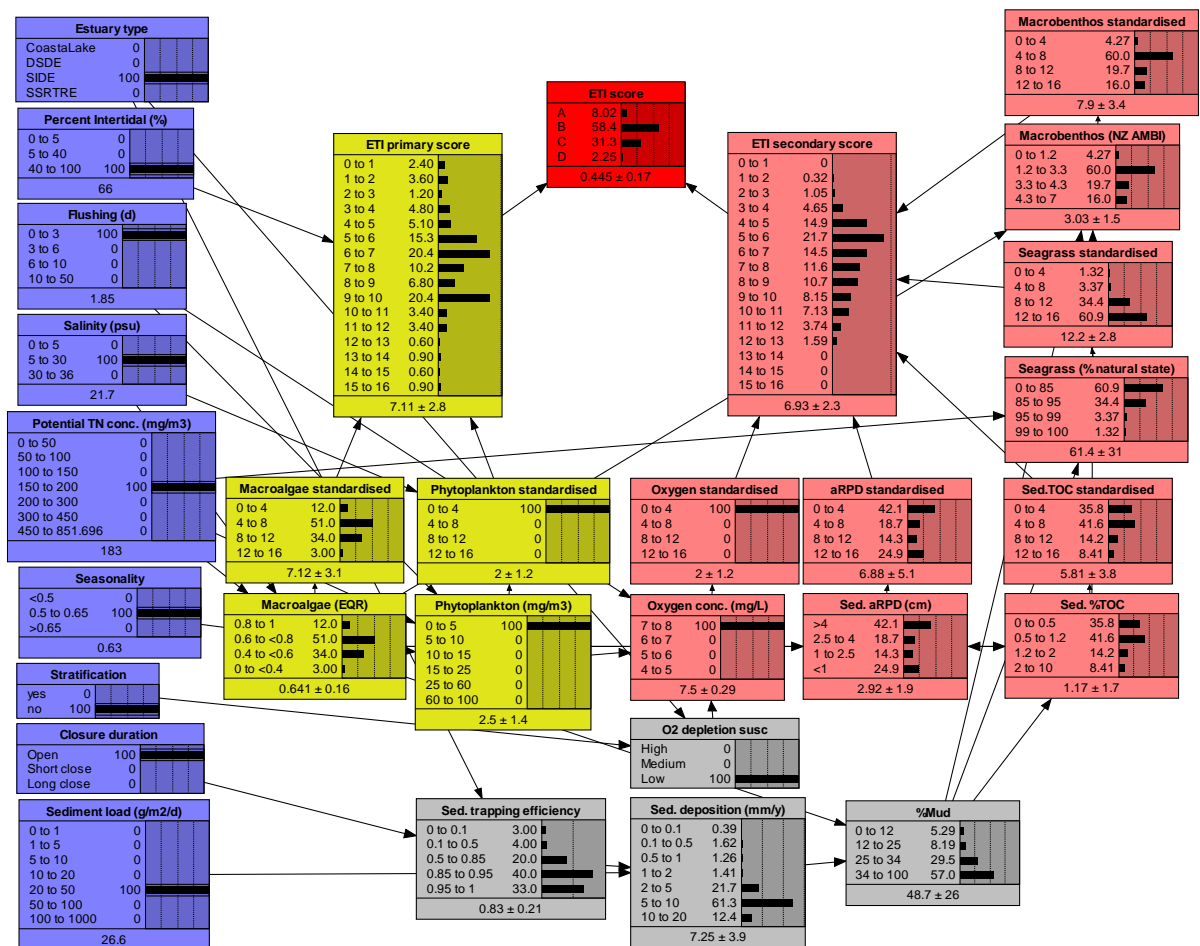


Figure 4-2: Netica BBN output for Jacobs River Estuary with potential TN concentration reduced by 66%.

Finally, we show an example for a lightly impacted estuary in its current state of potential TN concentration and sediment loading: Bluff Harbour (Southland), a SIDE – type estuary that is always open to the sea (Figure 4-3). Its probability distribution of results for ETI score is mainly in the A band, indicating an estuary with healthy conditions (Table 2-1). It has a low potential TN level, and very little sediment loading. Its macroalgal EQR value is high (minimal eutrophication), and its sediments have deep aRPD, and low %mud and %TOC. It is predicted to have healthy seagrass and good macrobenthos condition.

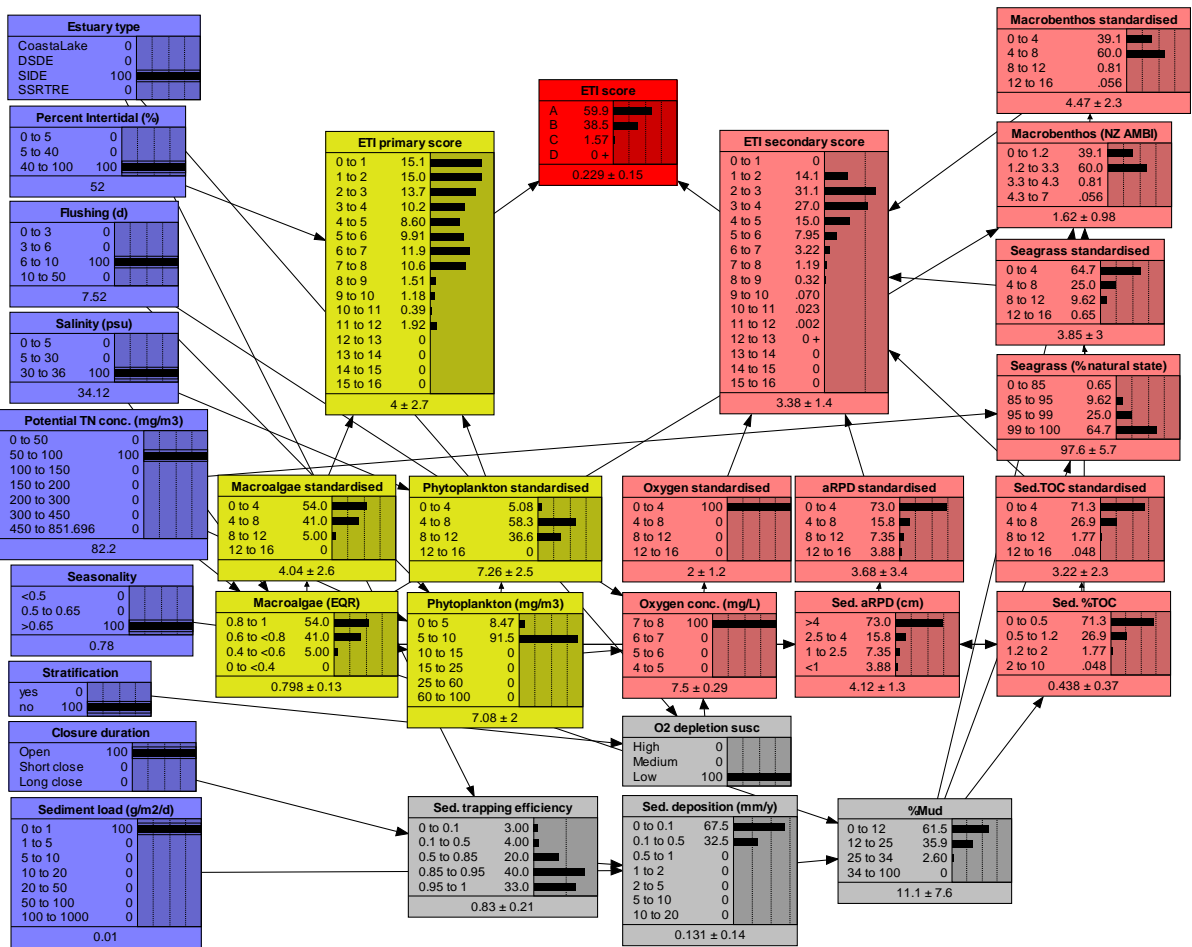


Figure 4-3: Netica BBN output for Bluff Harbour in its current state.

These example results demonstrate the utility of the ETI Tool 3 BBN. First, they show that multiple ecological indicators, as well as the final integrated ETI estuary health score, may be predicted solely based on the values of the drivers, which are readily available from ETI Tool 1 output. This means that estuary health status may be predicted in the absence of within-estuary indicator values should these not be available. Though not shown here, it is also true that should such indicator data be available, the BBN has the feature of allowing the user to update their respective nodes, which is expected to improve the accuracy of 'downstream' indicator predictions and the final ETI health score. Finally, the examples show how scenarios may be tested; perhaps most importantly, scenarios of how changed nutrient loading rates affect estuary health indices.

5 Acknowledgements

We thank Richard Storey (NIWA, Hamilton) for assistance with development of early versions of the ETI Tool 3 BBN and Leigh Stevens (Salt Ecology Ltd.) for provision of field data.

6 References

- Atkinson, M.J., and S.V. Smith. 1983. C:N:P ratios of benthic marine plants. *Limnology and Oceanography* 28: 568-574.
- Barr, N., J. Zeldis, K. Scheuer, and D. Schiel. 2020. Macroalgal Bioindicators of Recovery from Eutrophication in a Tidal Lagoon Following Wastewater Diversion and Earthquake Disturbance. *Estuaries and Coasts* 43: 240-255.
- Barr, N.G. 2007. Aspects of nitrogen metabolism in the green alga *Ulva*: developing an indicator of seawater nitrogen loading, University of Auckland.
- Batiuk, R., D. Breitburg, R. Diaz, T. Cronin, D. Secore, and G. Thursby. 2009. Derivation of habitat-specific dissolved oxygen criteria for Chesapeake Bay and its tidal tributaries. *Journal of Experimental Marine Biology and Ecology* 381: S204-S215.
- Batuik, R., P. Bergstrom, M. Kemp, E. Koch, L. Murray, C. Stevenson, R. Bartleson, V. Carter, N. Rybicki, J. Landwehr, C. Gallegos, L. Karrh, M. Naylor, D. Wilcox, K. Moore, M. Ailstock, and M. Teichberg. 2000. Chesapeake Bay Submerged Aquatic Vegetation Water Quality and Habitat-Based Requirements and Restoration Targets: A Second Technical Synthesis A Watershed Partnership.
- Booker, D.J., and R.A. Woods. 2014. Comparing and combining physically-based and empirically-based approaches for estimating the hydrology of ungauged catchments. *Journal of Hydrology (New Zealand)* 508: 227-239.
- Borja, A., J. Franco, V. Valencia, J. Bald, I. Muxika, M.J. Belzunce, and O. Solaun. 2004. Implementation of the European water framework directive from the Basque country (northern Spain): a methodological approach. *Marine Pollution Bulletin* 48: 209-218.
- Boynton, W., and W. Kemp. 2008. Estuaries. In *Nitrogen in the Marine Environment*, ed. D. Capone, D. Bronk, M. Mulholland and E. Carpenter, 809-856. Burlington, Massachusetts: Elsevier.
- Bricker, S., J. Ferreira, and T. Simas. 2003. An integrated methodology for assessment of estuarine trophic status. *Ecological Modelling* 169: 39-60.
- Burkholder, J., H.J. Glasgow, and J. Cooke. 1994. Comparative effects of water-column nitrate enrichment on eelgrass *Zostera marina*, shoalgrass *Halodule wrightii*, and widgeongrass *Ruppia maritima*. *Marine Ecology Progress Series* 105: 121-138.
- Burkholder, J.M., D.A. Tomasko, and B.W. Touchette. 2007. Seagrasses and eutrophication. *Journal of Experimental Marine Biology and Ecology* 350: 46-72.
- Cloern, J.E. 2001. Our evolving conceptual model of the coastal eutrophication problem. *Marine Ecology Progress Series* 210: 223-253.
- Cloern, J.E., and A.D. Jassby. 2008. Complex seasonal patterns of primary producers at the land-sea interface. *Ecology Letters* 11: 1294-1303.
- Conley, D.J., J. Carstensen, R. Vaquer-Sunyer, and C.M. Duarte. 2009. Ecosystem thresholds with hypoxia. *Hydrobiologia* 629: 21-29.
- Davies-Colley, R., P. Franklin, B. Wilcock, S. Clearwater, and C. Hickey. 2013. National Objectives Framework - Temperature, Dissolved Oxygen & pH Proposed thresholds for discussion. NIWA Client Report HAM2013-056. 83 pp.
- Duarte, C.M., and D. Krause-Jensen. 2018. Intervention Options to Accelerate Ecosystem Recovery From Coastal Eutrophication. *Frontiers in Marine Science* 5.
- Engelsen, A., S. Hulth, L. Pihl, and K. Sundbäck. 2008. Benthic trophic status and nutrient fluxes in shallow-water sediments. *Estuarine, Coastal and Shelf Science* 78: 783-795.
- Eppley, R. 1969. Half-saturation constants for uptake of nitrate and ammonium by marine phytoplankton. *Limnol Ocean* 14: 912-920.
- Ferreira, J.G., W.J. Wolff, T.C. Simas, and S.B. Bricker. 2005. Does biodiversity of estuarine phytoplankton depend on hydrology? *Ecological Modelling* 187: 513-523.

- Fong, P., R.M. Donohoe, and J.B. Zedler. 1994. Nutrient concentration in tissue of the macroalga *Enteromorpha* as a function of nutrient history - An experimental evaluation using field microcosms. *Marine Ecology-progress Series* 106: 273-281.
- Gibson, K., and I.D. Marsden. 2016. Seagrass *Zostera muelleri* in the Avon-Heathcote Estuary/Ihutai, summer 2015–2016. Estuarine Research Report 40 pp.
- Gray, J.S., R.S.-s. Wu, and Y.Y. Or. 2002. Effects of hypoxia and organic enrichment on the coastal marine environment. *Marine Ecology Progress Series* 238: 249-279.
- Green, L., M. Sutula, and P. Fong. 2014. How much is too much? Identifying benchmarks of adverse effects of macroalgae on the macrofauna in intertidal flats. *Ecological Applications* 24: 300-314.
- Harding, L.W., Jr., R.A. Batiuk, T.R. Fisher, C.L. Gallegos, T.C. Malone, W.D. Miller, M.R. Mulholland, H.W. Paerl, E.S. Perry, and P. Tango. 2014. Scientific Bases for Numerical Chlorophyll Criteria in Chesapeake Bay. *Estuaries and Coasts* 37: 134-148.
- Hicks, M., A. Semadeni-Davies, A. Haddadchi, U. Shankar, and D. Plew. 2019. Updated sediment yield estimator for New Zealand. NIWA Client Report 2018341CH. 190 pp.
- Huettel, M., and A. Rusch. 2000. Advective particle transport into permeable sediments—evidence from experiments in an intertidal sandflat. *Limnology and Oceanography* 45: 525-533.
- Hughes, B.B., J.C. Haskins, K. Wasson, and E. Watson. 2011. Identifying factors that influence expression of eutrophication in a central California estuary. *Marine Ecology Progress Series* 439: 31-43.
- Hume, T. 2018. Fit of the ETI trophic state susceptibility typology to the NZ coastal hydrosystems classification. NIWA Client Report 2017007CH. 34 pp. <https://shiny.niwa.co.nz/Estuaries-Screening-Tool-1/>
- Hume, T., P. Gerbeaux, D. Hart, H. Kettles, and D. Neale. 2016. A classification of New Zealand's coastal hydrosystems. NIWA Client Report HAM2016-062. 120 pp. <http://www.mfe.govt.nz/publications/marine/classification-of-new-zealands-coastal-hydrosystems>
- Hume, T.M., T. Snelder, M. Weatherhead, and R. Liefting. 2007. A controlling factor approach to estuary classification. *Ocean & Coastal Management* 50: 905-929.
- Hyland, J., L. Balthis, I. Karakassis, P. Magni, A. Petrov, J. Shine, O. Vestergaard, and R. Warwick. 2005. Organic carbon content of sediments as an indicator of stress in the marine benthos. *Marine Ecology Progress Series* 295: 91-103.
- Inglis, G.J. 2003. Seagrasses of New Zealand. In *World atlas of seagrasses*, ed. E.P. Green and F.T. Short, 134–143: University of California Press.
- Jones, H.F.E., C.A. Pilditch, D.A. Bruesewitz, and A.M. Lohrer. 2011. Sedimentary Environment Influences the Effect of an Infaunal Suspension Feeding Bivalve on Estuarine Ecosystem Function. *PLOS ONE* 6: e27065.
- Katwijk, M.M.v., L.H.T. Vergeer, G.H.W. Schmitz, and J.G.M. Roelofs. 1997. Ammonium toxicity in eelgrass *Zostera marina*. *Marine Ecology Progress Series* 157: 159-173.
- Kemp, M.W., R. Batleson, P. Bergstrom, V. Carter, Brendan R., C.L. Gallegos, W. Hunley, L. Karrh, E.W. Koch, J.M. Landwehr, K. Moore, A., L. Murray, M. Naylor, N.B. Rybicki, S.J. Court, and D.J. Wilcox. 2004. Habitat requirements for submerged aquatic vegetation in Chesapeake Bay: Water quality, light regime, and physical-chemical factors. *Estuaries* 27: 363-377.
- Kemp, W., Boynton WR, Adolphi JE, Boesch DF, Boicourt WC, Brush G, Cornwell JC, Fisher TR, Glibert PM, Hagy JD, Harding LW, Houde ED, Kimmel DG, Miller WD, Newell RIE, Roman MR, Smith EM, and Stevenson JC. 2005. Eutrophication of Chesapeake Bay: historical trends and ecological interactions *Marine Ecology Progress Series* 303: 1-29.
- Kemp, W., P. Sampou, J. Cafrey, M. Mayer, K. Henriksen, and W. Boynton. 1990. Ammonium recycling versus denitrification in Chesapeake Bay sediments. *Limnology and Oceanography* 35: 1545-1563.
- Lehninger, A. 1975. *Biochemistry*. New York: Worth Publishers.

- Lohrer, A., S. Thrush, and M. Gibbs. 2004. Bioturbators enhance ecosystem function through complex biogeochemical interactions. *Nature* 431: 1092–1095.
- Lohrer, A.M., J.E. Hewitt, and S.F. Thrush. 2006. Assessing far-field effects of terrigenous sediment loading in the coastal marine environment. *Marine Ecology Progress Series* 315: 13-18.
- Martins, I., J.M. Oliveira, M.R. Flindt, and J.C. Marques. 1999. The effect of salinity on the growth rate of the macroalgae *Enteromorpha intestinalis* (Chlorophyta) in the Mondego estuary (west Portugal). *Acta Oecologica* 20: 259-265.
- Matheson, F., and S. Wadhwa. 2012. Seagrass in Porirua Harbour Preliminary assessment of restoration potential. NIWA Client Report HAM2012-037. 35.
- Ministry for the Environment. 2018. A Guide to Attributes in Appendix 2 of the National Policy Statement for Freshwater Management (as amended 2017). Wellington: Ministry for the Environment.
- Monbet, Y. 1992. Control of Phytoplankton Biomass in Estuaries: A Comparative Analysis of Microtidal and Macrotidal Estuaries. *Estuaries* 15: 563–571.
- Morrison, M., M. Lowe, D. Parsons, N. Usmar, and I. McLeod. 2009. A review of land-based effects on coastal fisheries and supporting biodiversity in New Zealand. New Zealand Aquatic Environment and Biodiversity Report 100 pp.
- Norsys. 2005. Netica™ Application: A complete software application to solve problems using Bayesian belief Networks and influence diagrams. <http://www.norsys.com>
- NRC. 2000. *Clean Coastal Waters understanding and reducing the effects of nutrient pollution*. Washington DC: National Academy Press.
- Orth, R.J., W.C. Dennison, C. Gurbisz, M. Hannam, J. Keisman, J.B. Landry, J.S. Lefcheck, K.A. Moore, R.R. Murphy, C.J. Patrick, J. Testa, D.E. Weller, D.J. Wilcox, and R.A. Batiuk. 2019. Long-term Annual Aerial Surveys of Submersed Aquatic Vegetation (SAV) Support Science, Management, and Restoration. *Estuaries and Coasts*.
- Park, S., and R. Donald. 1994. Environment Bay of Plenty Tauranga Harbour Regional Plan Environmental Investigations. Ecology of Tauranga Harbour. Environment Bay of Plenty Environmental Report 94/8. 177 pp.
- Park, S.G. 1999. Changes in abundance of seagrass (*Zostera* spp.) in Tauranga Harbour from 1959 – 96. Environment Bay of Plenty Environmental Report 99/30. 19 pp.
- Pelletier, M.C., D.E. Campbell, K.T. Ho, R.M. Burgess, C.T. Audette, and N.E. Detenbeck. 2011. Can sediment total organic carbon and grain size be used to diagnose organic enrichment in estuaries? *Environmental Toxicology and Chemistry* 30: 538-547.
- Plew, D., B. Dudley, and U. Shankar. 2020a. Eutrophication susceptibility assessment of Toetoes (Fortrose) Estuary. NIWA Client Report 2020070CH. 58 pp
- Plew, D.R., J.R. Zeldis, B.D. Dudley, A.L. Whitehead, L.M. Stevens, B.M. Robertson, and B.P. Robertson. 2020b. Assessing the Eutrophic Susceptibility of New Zealand Estuaries. *Estuaries and Coasts* 43: 2015-2033.
- Plew, D.R., J.R. Zeldis, U. Shankar, and A.H. Elliott. 2018. Using simple dilution models to predict New Zealand estuarine water quality. *Estuaries and coasts* 41: 1643-1659.
- Pratt, D.R., A.M. Lohrer, C.A. Pilditch, and S.F. Thrush. 2014. Changes in Ecosystem Function Across Sedimentary Gradients in Estuaries. *Ecosystems* 17: 182-194.
- Quinn, J.M., R.M. Monaghan, V.J. Bidwell, and S.R. Harris. 2013. A Bayesian Belief Network approach to evaluating complex effects of irrigation-driven agricultural intensification scenarios on future aquatic environmental and economic values in a New Zealand catchment. *Marine and Freshwater Research* 64: 460-474.
- Reynolds, L.K., M. Waycott, K.J. McGlathery, and R.J. Orth. 2016. Ecosystem services returned through seagrass restoration. *Restoration Ecology* 24: 583-588.
- Robertson, B., P. Gillespie, R. Asher, S. Frisk, N. Keeley, G. Hopkins, S.J. Thompson, and B.J. Tuckey. 2002. Estuarine Environmental Assessment and Monitoring, A National Protocol. Part A.

- Development, Part B. Appendices and Part C. Application. Sustainable Management Fund Contract No.5096. Part A. 93p. Part B. 159p. Part C 40p plus field sheets.
- Robertson, B., and C. Savage. 2018. Mud-entrained macroalgae utilise porewater and overlying water column nutrients to grow in a eutrophic intertidal estuary. *Biogeochemistry* 139: 53-68.
- Robertson, B., L. Stevens, B. Robertson, J. Zeldis, M. Green, A. Madarasz-Smith, D. Plew, R. Storey, T. Hume, and M. Oliver. 2016a. NZ Estuary Trophic Index Screening Tool 1. Determining eutrophication susceptibility using physical and nutrient load data. Prepared for Envirolink Tools Project: Estuarine Trophic Index, MBIE/NIWA Contract No: C01X1420 47 pp.
- Robertson, B., L. Stevens, B. Robertson, J. Zeldis, M. Green, A. Madarasz-Smith, D. Plew, R. Storey, T. Hume, and M. Oliver. 2016b. NZ Estuary Trophic Index Screening Tool 2. Determining Monitoring Indicators and Assessing Estuary Trophic State. Prepared for Envirolink Tools Project: Estuarine Trophic Index, MBIE/NIWA Contract No: C01X1420 68 pp.
- Robertson, B.M., L.M. Stevens, N. Ward, and B.P. Robertson. 2017. Condition of Southland's Shallow, Intertidal Dominated Estuaries in Relation to Eutrophication and Sedimentation: Output 1: Data Analysis and Technical Assessment - Habitat Mapping, Vulnerability Assessment and Monitoring Recommendations Related to Issues of Eutrophication and Sedimentation. Report prepared by Wriggle Coastal Management for Environment Southland 172 pp.
- Robertson, B.P., J.P.A. Gardner, and C. Savage. 2015. Macrobenthic–mud relations strengthen the foundation for benthic index development: A case study from shallow, temperate New Zealand estuaries. *Ecological Indicators* 58: 161-174.
- Robertson, B.P., C. Savage, J.P.A. Gardner, B.M. Robertson, and L.M. Stevens. 2016c. Optimising a widely-used coastal health index through quantitative ecological group classifications and associated thresholds. *Ecological Indicators* 69: 595-605.
- Scully, M.E. 2016. The contribution of physical processes to inter-annual variations of hypoxia in Chesapeake Bay: A 30-yr modeling study. *Limnology and Oceanography* 61: 2243-2260.
- Sheldon, J., and M. Alber. 2010. The condition of Georgia's coastal waters: development and analysis of water quality indicators. Georgia Coastal Research Council 173.
- Snelder, T.H., A.L. Whitehead, C. Fraser, S.T. Larned, and M. Schallenberg. 2020. Nitrogen loads to New Zealand aquatic receiving environments: comparison with regulatory criteria. *New Zealand Journal of Marine and Freshwater Research* 54: 1-24.
- Stevens, L.M. 2018a. New River Estuary: 2018 Macroalgal Monitoring. Report prepared by Wriggle Coastal Management for Environment Southland 29 pp.
- Stevens, L.M. 2018b. Whanganui Inlet : Mapping of Historical Seagrass Extent. 10 pp.
- Stevens, L.M., and B.P. Robertson. 2017. Fortrose (Toetoes) Estuary 2016: Broad Scale Substrate, Macroalgae and Seagrass Mapping. Report prepared by Wriggle Coastal Management for Environment Southland 28 p.
- Sutula, M. 2011. Review of Indicators for Development of Nutrient Numeric Endpoints in California Estuaries. Southern California Coastal Water Research Project Technical Report 269.
- Sutula, M., H. Bailey, and S. Poucher. 2012. Science Supporting Dissolved Oxygen Objectives in California Estuaries. Southern California Coastal Water Research Project Technical Report 684. 86 pp.
www.sccwrp.org/pub/download/DOCUMENTS/TechnicalReports/684_DO_NNE.pdf
- Sutula, M., L. Green, G. Cicchetti, N. Detenbeck, and P. Fong. 2014. Thresholds of Adverse Effects of Macroalgal Abundance and Sediment Organic Matter on Benthic Habitat Quality in Estuarine Intertidal Flats. *Estuaries and Coasts* 37: 1532-1548.
- Townsend, M., and D. Lohrer. 2015. ANZECC Guidance for Estuary Sedimentation. NIWA Client Report HAM2015-096. 45 pp.
- Uusitalo, L. 2007. Advantages and challenges of Bayesian networks in environmental modelling. *Ecological Modelling* 203: 312-318.
- Vaquar-Sunyer, R., and C.M. Duarte. 2008. Thresholds of hypoxia for marine biodiversity. *Proc Natl Acad Sci USA* 105: 15452-15457.

- Vaquer-Sunyer, R., and C.M. Duarte. 2011. Temperature effects on oxygen thresholds for hypoxia in marine benthic organisms. *Global Change Biology* 17: 1788-1797.
- Wallace, R.B., H. Baumann, J.S. Grear, R.C. Aller, and C.J. Gobler. 2014. Coastal ocean acidification: The other eutrophication problem. *Estuarine, Coastal and Shelf Science* 148: 1-13.
- WFD-UKTAG. 2014. UKTAG Transitional and Coastal Water Assessment Method Macroalgae Opportunistic Macroalgal Blooming Tool. <http://www.wfduk.org/sites/default/files/Media/>
- Whitehead, A., C. Depree, and J. Quinn. 2019. Seasonal and temporal variations in water quality in New Zealand rivers. Prepared for Ministry for the Environment 2019024CH. 79. <https://www.mfe.govt.nz/publications/fresh-water/seasonal-and-temporal-variation-water-quality-new-zealand-rivers-and-lakes>
- Zabarte-Maeztu, I., F. Matheson, I. Hawes, and M. Manley-Harris. 2019. Sediment-effect thresholds for the seagrass, *Zostera muelleri*: a case study in Porirua Harbour, New Zealand. In New Zealand Marine Sciences Society Conference. Dunedin.
- Zeldis, J., R. Measures, L. Stevens, F. Matheson, and B. Dudley. 2019. Remediation Options for Southland Estuaries. NIWA Client Report 2019344CH. 73. <https://contentapi.datacomsphere.com.au/v1/h%3Aes/repository/libraries/id:26gi9ayo517q9stt81sd/hierarchy/document-library/reports/science-reports/Remediation%20Options%20for%20Southland%20Estuaries%202019.pdf>
- Zeldis, J., D. Plew, A. Whitehead, A. Madarasz-Smith, M. Oliver, L. Stevens, B. Robertson, O. Burge, and B. Dudley. 2017a. The New Zealand Estuary Trophic Index (ETI) Tools: Tool 1 - Determining Eutrophication Susceptibility, Ministry of Business, Innovation and Employment Envirolink Tools Contract : C01X1420
- Zeldis, J., R. Storey, D. Plew, A. Whitehead, A. Madarasz-Smith, M. Oliver, L. Stevens, B. Robertson, and B. Dudley. 2017b. The New Zealand Estuary Trophic Index (ETI) Tools: Tool 3 - Assessing Estuary Trophic State using a Bayesian Belief Network Ministry of Business, Innovation and Employment Envirolink Tools Contract: C01X1420.
- Zeldis, J., A. Swales, K. Currie, K. Safi, S. Nodder, C. Depree, F. Elliott, M. Pritchard, M. Gall, J. O'Callaghan, D. Pratt, S. Chiswell, M. Pinkerton, D. Lohrer, and S. Bentley. 2015. Firth of Thames Water Quality and Ecosystem Health – Data Report. NIWA Client Report CHC2014-123. 177 pp. <http://www.waikatoregion.govt.nz/tr201523/>
- Zeldis, J., A. Whitehead, D. Plew, A. Madarasz-Smith, M. Oliver, L. Stevens, B. Robertson, R. Storey, O. Burge, and B. Dudley. 2017c. The New Zealand Estuary Trophic Index (ETI) Tools: Tool 2 - Assessing Estuary Trophic State using Measured Trophic Indicators, Ministry of Business, Innovation and Employment Envirolink Tools Contract: C01X1420.
- Zeldis, J.R., C. Depree, C. Gongol, P.M. South, A. Marriner, and D.R. Schiel. 2020. Trophic Indicators of Ecological Resilience in a Tidal Lagoon Estuary Following Wastewater Diversion and Earthquake Disturbance. *Estuaries and Coasts* 43: 223-239.
- Zeldis, J.R., and D.P. Swaney. 2018. Balance of Catchment and Offshore Nutrient Loading and Biogeochemical Response in Four New Zealand Coastal Systems: Implications for Resource Management. *Estuaries and Coasts* 41: 2240-2259.